METRANS RESEARCH PROJECT

Project 01-10

Smart Damping for Monitoring the Health of Bridge Structures

FINAL REPORT

June 2003

Prof. Erik A. Johnson
Principal Investigator, Assistant Professor
Department of Civil and Environmental Engineering
University of Southern California

Mohamed I.S. Elmasry
Graduate Research Assistant
Department of Civil and Environmental Engineering
University of Southern California

PARAMETRIC FREQUENCY DOMAIN IDENTIFICATION USING VARIABLE STIFFNESS AND DAMPING DEVICES

Prof. Erik A. Johnson
Principal Investigator, Assistant Professor
Department of Civil and Environmental Engineering
University of Southern California

Mohamed I.S. Elmasry
Graduate Research Assistant
Department of Civil and Environmental Engineering
University of Southern California

June 2003

ABSTRACT

Accurate diagnosis of structural health is a vital step in protecting structures. Whether caused by acute events, such as earthquakes or other natural disasters, or long-term degradation from environment and human use (and abuse), structural damage can threaten both human life and economic loss. An autonomous monitoring system that has the capability of predicting the location of damage would have a positive economic impact, not to mention the potential for saving lives by giving quick assessments of structural health and whether immediate evacuation of, or re-routing, around a structure is necessary. The process of monitoring structural health and identifying damage severity and location is generally termed *structural health monitoring* (SHM). The core of this project is to investigate how variable stiffness and damping devices (VSDD) can be most effectively used to identify local damage in bridge and building structures. Using one or more VSDDs to modify the response, simulated damage is detected, localized, and quantified. One fundamental goal is to determine the best VSDD actions — whether adding damping or stiffness — to precisely and robustly locate and identify bridge damage. This study is based on simulation of bridge motion and other structures due to ambient excitation sources. Several VSDD behaviors, such as variable stiffness mode and variable damping mode, are studied in the context of a frequency domain analysis. These analyses are performed on simple models of bridge and building dynamics, *e.g.*, two degree-of-freedom (2DOF) shear model systems and a six degree-of-freedom (6DOF) model. Structural behavior is assumed locally linear before damage and after damage. Generally, VSDDs were successful in improving the damage identification in structures using the variable stiffness mode but rather unsuccessful in the variable damping only mode. In addition to demonstrating the potential of using variable stiffness and damping devices to improve structural health monitoring, this study also provides some insights into further avenues of future research to build on the improvements studied herein.

Keywords: structural health monitoring, variable stiffness and damping devices, parametric frequency-domain identification, damage detection, structural control.

TABLE OF CONTENTS

TABLE OF FIGURES

LIST OF TABLES

DISCLAIMER

The contents of this report reflect the views of the authors, who are responsible for the facts and the accuracy of the information presented herein. This document is disseminated under the sponsorship of the Department of Transportation, University Transportation Centers Program, and California Department of Transportation in the interest of information exchange. The U.S. Government and California Department of Transportation assume no liability for the contents or use thereof. The contents do not necessarily reflect the official views or policies of the State of California or the Department of Transportation. This report does not constitute a standard, specification, or regulation.

ACKNOWLEDGMENTS

The authors gratefully acknowledge the partial support of this work by Caltrans through the National Center for Metropolitan Transportation Research (METRANS), and by the National Science Foundation under CAREER grant 00-94030.

.

1.0 INTRODUCTION

Accurate diagnosis of structural health is a vital step in protecting structures. Whether caused by acute events, such as earthquakes or other natural disasters, or long- term degradation from environmental effects and human use (and abuse), structural damage can threaten both danger to human life and economic loss. The process of monitoring structural health and identifying damage existence, severity and location is generally termed *structural health monitoring* (SHM). Chang (1999) defined structural health monitoring to be an "autonomous [system] for the continuous monitoring, inspection, and damage detection of [a structure] with minimum labor involvement."

Structural health monitoring has long been recognized as its own particular category within system identification whose area is well established. High fidelity modeling and accurate response estimation are required for SHM for several reasons, foremost being the monitoring of structural characteristics and response to predict the onset of failure or the expected remaining life, and for the purposes of controlling the motion of the structure.

By determining the model that best fits data taken from the structure, certain structural characteristics may be identified. With identification at different points in time — periodic or shortly after natural disasters — changes in these characteristics may be monitored. With damage models, changes in structural characteristics are used to predict damage severity and location.

This report proposes using smart, controllable passive devices such as Variable Stiffness and Damping devices (VSDDs) in structures to improve SHM, and demonstrates the benefits over conventional passive structures.

1.1 SHM Benefits

Clear needs for structural health monitoring exist for both building and bridge structures. For example, significant expenditures after the 1994 Northridge earthquake went to inspecting joints of steel buildings for damage. These joints are often hidden within a structure, such as behind walls or encased in concrete (for example, see Figs. 1–3), and require removal of non-structural material, not to mention putting (at least part of) the structure out of service during inspection. Similar expenditures were required after the 1995 Hyogo-Ken Nanbu (Kobe) earthquake as well (Mita, 1999). A recent report to the U.S. Congress by the Federal Highway Administration (FHWA, 2002) indicates that approximately 25% of the bridges in the U.S. are rated as deficient. It is estimated that it will require an investment of 7 billion dollars per year for the next two decades to rebuild or replace the bridge infrastructure in the U.S. (Patten *et al.*, 1999). This all when many public budgets are in the billions of dollars in the red (EBBT, 2002). All of these facts make clear the essential need for effective structural health monitoring systems.

1.2 Difficulties of Conventional SHM Approaches

One approach to SHM is based on global vibration methods. In applying these methods, many global vibration SHM studies assume a class of mathematical models that may represent the actual structure. When considering damage detection, these studies have focused on identifying changes in of modal parameters, such as natural frequencies, mode shapes, and modal damping ratios, obtained from measured vibration response. Recent state-of-the-art surveys of global vibration SHM techniques applied to civil engineering applications are given by Doebling *et al.* (1996, 1998).

Figure 1. Beam-column connection damage (Kiremedjian, 1999)

Figure 2. Plastic hinging at top of column (Hall, 1995)

Figure 3. Cracks through column flange and extending into web (Hall, 1995)

Unfortunately, no global technique has been well established and accepted as an overall successful approach (Sanayei *et al*., 1998). Some explanatory reasons are that (*i*) models cannot perfectly predict the full behavior of real structures, (*ii*) periodic environmental effects such as thermally-induced variations may mask the effects of damage on global vibration characteristics, (*iii*) measurement noise can cause significant variation from one test to the next, (*iv*) excitation is limited to ambient sources for most civil structures, and (*v*) sensitivity of global vibration characteristics to damage may be small. These can all lead to variations in the identified model parameters characteristics that are not due to true changes in the structure, raising uncertainty in damage estimates (Vanik *et al*., 2000).

Using forced structural response strategies can overcome some of the aforementioned problems. For example, forced response interrogation can be timed to minimize periodic environmental effects from one test to the next, and may provide greater excitation energy to decrease signal-to-noise ratios in comparison with ambient excitation. For structures with embedded active vibration control systems, the actuators can be used to enhance damage detection by tuning the actuation signals to directly increase closed-loop damage sensitivity of global vibration characteristics (Ray and Tian, 1999).

In spite of the advantages of using forced response, large actuation devices are not being used in a continuous manner for civil structures (except a few isolated cases in Asia) due to the large power requirements, concerns about stability and so forth, rendering them impractical for damage mitigation or SHM of civil structures. Further, building and bridge owners typically prefer their structures not to be shaken deliberately, both for comfort of occupants or users of the structures and to lessen any chance of risking further damage.

Given these limitations, one is restricted to analyzing response to ambient excitation to perform SHM. Ambient excitation on bridge structures takes a number of forms including wind, traffic, waves and microtremors. The ambient excitation approach has several advantages over approaches using forced vibration response. For example, for the low amplitude excitations typically experienced during ambient vibration, most structural systems are well characterized with linear models. In addition, continuous ambient vibration tests can be performed at a very low cost. However, while applications of ambient excitation identification techniques are more acceptable than active control ones, the sensitivity of the measured signals to noise is a pressing question. Due to small structural response under such ambient excitations, the signal-to-noise ratios are small enough to make SHM difficult and results uncertain. Thus, solutions to these SHM difficulties must be sought elsewhere.

1.3 Use VSDDs to Improve SHM

One approach that may help alleviate some of the SHM difficulties for civil structures would be to use "smart" variable stiffness and damping devices (VSDDs) — controllable passive devices that have received significant study for vibration mitigation (Spencer and Sain, 1997; Symans and Constantinou, 1999) — in a synergistic manner to provide internal parametric changes to affect sensitivity to damage. VSDDs are already being used to improve the performance of structures subjected to natural hazards by mitigating vibration response. In addition to providing near optimal structural control strategies for vibration mitigation, these low-power and fail-safe devices can also provide parametric changes to increase global vibration measurement sensitivity for health monitoring. Further, the integration of smart damping and health monitoring can exploit, in a synergistic manner, the common aspects of both technologies as seen in the flowcharts in Fig. 4.

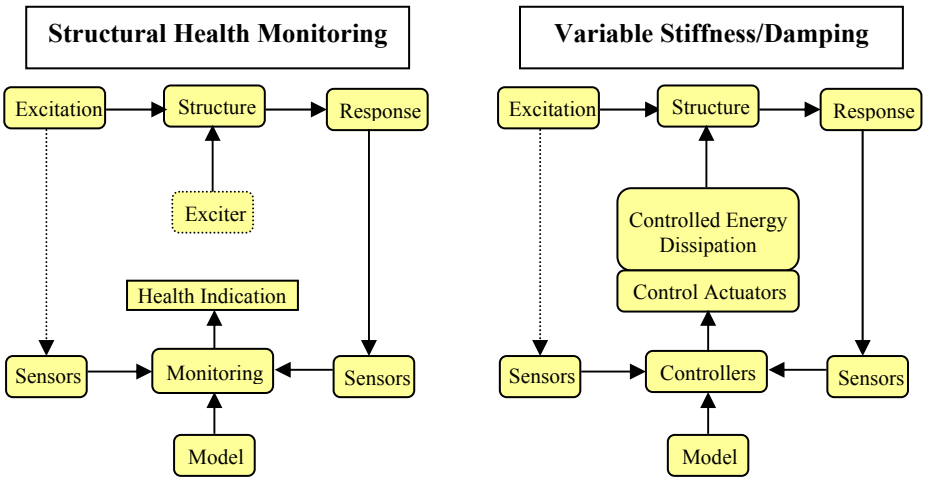

Figure 4. SHM and variable stiffness/damping flow charts

VSDDs can adjust the behavior of a structure by real-time modification of stiffness and damping at discrete points within the structure. By commanding different behavior for each VSDD in a structure, multiple structural configurations can be tested, each of which can be designed to increase the sensitivity to damage in different portions of the structure (see Fig. 5). For example, consider a structure with four stiffness devices with "on" and "off" settings; there are 2^4, or 16, distinct configurations, each of which can provide some information about the structural characteristics. The SHM is provided, then, with multiple signatures of the structure, each of which can provide additional and, if done efficiently, mostly complementary information. As an analogy to the previous discussion, consider taking a sequence of photographs of the front of a house. If the camera is exactly in front of the house for each picture, relatively little depth information can be gathered. However, shifting the camera (or changing the lighting) can give computer modeling software significantly new complementary information.

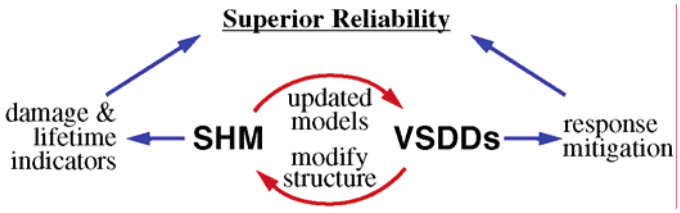

Figure 5. Mutual benefits of SHM and VSDDs

1.4 Overview of this VSDD/SHM Research Project

This report proposes using VSDDs in structures to improve SHM, and demonstrates the benefits in contrast with conventional passive structures. Several structures are studied herein, with one or more VSDDs installed. First 2DOF and then 6DOF shear structural models are studied, each in several configurations: the 2DOF structure with a VSDD in (*i*) the first story, (*ii*) the second story, and (*iii*) both stories, and the 6DOF building with VSDDs in the first three stories. Then, a 2DOF bridge structure model (Erkus *et al.*, 2002) is studied with a VSDD attached in the bearing layer between the pier and the deck. In each case, the VSDD is chosen to act as an ideal variable stiffness/damping device, with one of several discrete stiffness/damping values. Some examples from simulation are used to demonstrate the benefits of the proposed method.

The focus herein is introducing a better approach for estimating the structural dynamic parameters through the use of variable stiffness and damping devices. Since controllable stiffness/damping devices are used to give the parametric changes necessary for improved monitoring, the bridge models must be *control-oriented* dynamic models — *i.e.*, low-order models that still capture most of the salient dynamic characteristics of a real bridge, particularly in the locations of the controllable devices and in the frequency ranges driven by the excitation. These devices are located in the structures in the form of lateral bracing or, in the bridge example, in the isolation layer between the bridge deck and the pier supports. It is assumed that transfer functions from ground acceleration to absolute horizontal accelerations of the different degrees-of-freedom have been determined experimentally through standard procedures with the VSDDs at various stiffness or damping settings. Herein, these transfer functions are modeled by the exact transfer functions plus the Fourier transform of a Gaussian pulse process that would be typical of band-limited Gaussian white sensor noise vector processes. A conventional least-squares approach is adopted to estimate structural parameters. Because of the VSDDs' useful

properties, they were able to improve the sensitivity of the identification. It is shown that using variable stiffness devices in a structure subjected to repetitive ambient vibration simulation, favorable results are obtained compared to other approaches.

While the VSDD approach can be used with other identification methods, it is here investigated in the context of a parametric frequency domain identification to determine structural parameters. Historically, frequency-domain approaches have dominated modal testing literature for many years. In the vast majority of modal testing, frequency response functions are measured prior to using a modal identification algorithm (Juang, 1994). Experienced modal testing personnel can deduce considerable information by examining frequency response functions.

In this report, conventional parametric identification in the frequency domain is described. The direct transfer function polynomial identification is rather complex in the unknown parameters. Consequently, one simplification discussed in the literature is explained. However, it is shown that this simplification can often lead to significant bias in parameter estimates due to unwanted magnification of sensor noise effects. The numerical examples herein use a fairly noisy signal to challenge the methods. An iterative method is proposed that approximates the more direct method. These methods are then applied to conventional structural identification, assuming no VSDD within the structure, and then with VSDDs using several distinct stiffness settings and (later) distinct damping settings.

It is shown that using the least squares approach on the modified version of the error in transfer functions with known starting guesses, both using VSDD and conventional identification techniques give parameter estimates. The latter gives similar mean estimates but the VSDDs approach gives rather smaller variation. For biased starting guesses, the VSDDs approach gives more accurate estimate means than the conventional approach though with slightly larger variation.

The choice of VSDD location(s), possibly key to efficient algorithms, is also important. Though it seems beneficial to include these devices in all stories, cost benefit analysis (of SHM as well as hazard vibration mitigation) may indicate that using fewer devices is more economical. Accordingly, in the 6DOF model studied herein, one VSDD is assumed in each of the first three structural segments only. The results show again the effectiveness of adding these devices in improving the mean estimates of the structural parameters and their variations, even with a quite noisy measurement signal.

In summary, this report documents a study that demonstrates the potential of improving SHM by exploiting the controllable properties of variable stiffness and damping devices. Further, the study raised additional questions and insights that should be investigated in future research. These conclusions and future directions comprise the last chapter of the report.

2.0 LITERATURE REVIEW

The field of structural health monitoring has been quite rich with research in the last few decades. The impact and benefits, both economic and societal, of SHM have drawn the interest of many researchers. The results of relevant work in the literature can be loosely broken down into several related categories; some representative examples in each category are briefly highlighted in this chapter. First, an overview of SHM approaches is given, followed by a discussion of modeling issues. Then several classes of system identification methods are described. Finally, variable stiffness and damping devices are reviewed, highlighting the various types and some applications in which they have been studied.

2.1 Research on Structural Health Monitoring

Conventional research in SHM and damage detection for civil structures can be roughly classified into local and global methods. Local SHM methods detect changes in a structure in localized regions using, for example, ultrasound, x-ray, piezoelectric devices and so forth. Unfortunately, local SHM methods have limited range; *e.g.*, piezoelectric devices have an effective range on the order of 30 cm (Wang and Chang, 1999). For large civil structures, this would require a staggering number of devices to monitor the entire structure. Furthermore, other local methods usually require significant human involvement or are limited to areas where damage might be expected to occur. Consequently, service costs and errors in expected damage locations limit the usefulness of such methods.

Conventional global vibration SHM methods (Doebling *et al.*, 1996, 1998) typically focus on identifying changes in modal parameters (*e.g.*, natural frequencies, mode shapes, and modal damping ratios) computed from measured vibration response. With identification at different points in time — periodic or shortly after natural disasters — changes in these characteristics may be monitored. However, these approaches also have their difficulties. Global methods based on ambient excitation are easy to implement as they require no additional excitation source, but simply may not reveal certain defects since some damage mechanisms are only strongly observable with narrowband excitation that ambient sources alone cannot provide. Using known excitation with force actuators can overcome this difficulty but, with a few exceptions in Asia, such active devices are not used in civil structures for other purposes so widespread permanent installation and use is unlikely. As a result, no global technique has been well established and accepted as an overall successful approach (Sanayei *et al.*, 1998).

A benchmark study in structural health monitoring based on simulated structural response data was developed by the joint IASC-ASCE task group on structural health monitoring. This benchmark was created to facilitate a comparison of various methods employed for the health monitoring of structures. The focus of the problem is simulated acceleration response data from an analytical model of an existing physical structure. This problem was addressed and studied by various researchers including Au *et al.* (2000), Bernal and Gunes (2000), Caicedo *et al*. (2003), Corbin *et al.* (2000), Johnson *et al.* (2003), Katafygiotis *et al*. (2000) and Luş and Betti (2000). This SHM benchmark problem, both the definition and the application of a number of SHM methods to solve the problem, will be published a special issue of the Journal of Engineering Mechanics later in 2003.

SHM approaches, particularly ones based on global vibration, often involve some level of structural modeling and some type of system identification. The modeling, which is described in

more detail in the following section, whether discrete or continuous in nature, has the difficulty that no model has the exact same dynamic properties as the structure it is intended to represent. Fortunately, the small motion levels typical of ambient vibration response can alleviate some of these issues. In addition to various modeling approaches, there are numerous system identification techniques, some of which are described in the third section of this chapter.

2.2 Modelling of Structures for SHM

Picking the right model to represent a particular structure has been a critical issue in the application of SHM. Capecchi and Vestroni (1999) state that, from a theoretical point of view, it is convenient to distinguish between continuous and discrete structures. Although all structures are in fact continuous, structures in which concentrated masses are dominant are considered discrete in dynamic analysis. In the context of damage identification, structures are considered as discrete if the damage cannot affect a portion smaller than the element. Thus frames, for example, are seen as discrete structures whereas bridge decks and pipelines are usually considered continuous. For continuous structures, it is conceptually correct to pose the problem of localizing of a crack, because its position affects the entire dynamics. For a discrete structure the problem is different; for example, it is not possible to precisely determine where, in an element, a crack exists because the structure is modeled discretely, with all characteristics of the element taken as a whole.

Despite extensive research in modeling, structural models cannot be expected to perfectly predict the full behavior of the structure. For example, the model may not account for effects such as thermally-induced daily variations and amplitude dependence of modal parameters. Further, the available measured information is restricted by limits on the amount of instrumentation. Nonlinearities are also a major obstacle where the model becomes very difficult to implement and each nonlinear system is a special case of its own. Moreover, while finite element modeling is convenient, it often produces a dynamic model that neither is of modest order nor accurately captures the dynamics of the built structure. Some reasons for the latter are mismodelling of structural elements, differences between actual and modeled material properties and dimensions, approximation in finite element derivations, and poor convergence of the numerical model (Juang, 1994). For SHM, models of extremely high order are of limited utility as, often, only a small number of the lower modes of a structure can be identified with confidence (Beck *et al.*, 2001). Additionally, a real structure often has nonlinearities and higher frequency modes (or local vibration modes) that may be missed in the analytical modeling, leading to what is generally termed "model error." All of these difficulties make clear the complexity of the modeling problem.

Using ambient vibration to excite structures may simplify the modeling problem necessary for SHM. Basically, the model can be considered linear in that case (see, *e.g.*, Beck *et al.*, 2001). This assumption is based upon the facts that ambient excitations are small, and that civil structures are highly rigid, making them behave linearly under small external excitations. Linear behavior, as well as safety considerations, have encouraged numerous researchers to adopt ambient excitation approaches in SHM.

2.3 System Identification for SHM

As there is no unique and general mathematical definition for damage, researchers tend to relate damage to changes in structural model parameters (such as stiffness, damping, and masses)

or sometimes modal parameters (such as natural frequencies and mode shapes). This may be done by assigning damage indices that are functions of the structural parameters or by evaluating the damage as the reduction in one or more of these parameters. Accordingly, identifying these parameters, whether modal or model parameters, is crucial for SHM application. Unfortunately, these parameters cannot be easily or directly mathematically derived from structural response but rather require extensive measurements and signal processing that are generally termed *system identification* techniques. System identification is the process of developing or improving a mathematical representation of a physical system using experimental data (Juang, 1994). Thereafter, this model is used to estimate the properties of the dynamic system such as stiffness, damping, frequencies, etc., through computational techniques that use the known input/output data.

System Identification (SI) techniques to study the actual states of civil engineering structures have received considerable attention in recent years, as extensive full-scale experimental studies are expensive and often difficult to perform. Identification techniques are divided into frequency domain and time domain methods. Some of the key approaches among these techniques are discussed in the next two sections, followed by brief summaries of ERA/subspace approaches and some research in the literature focused specifically on structural model parameter identification (both of which can be studied in the frequency or time domains).

2.3.1 Frequency Domain Techniques

Frequency-domain identification (parametric/non-parametric) techniques in control engineering and system identification gained relevance with stability and design methods based on frequency response measurements (Juang, 1994). This approach began with the technique known as transfer function (TF) analysis. Many frequency dependent methods, such as the empirical transfer-function estimate (ETFE), bootstrap methods, separable least squares methods, etc., are detailed by Ljung (1999).

One of the first methods that used the frequency domain data in the identification of the transfer function (TF) of the system was attributed to the efforts by Levy (1959). Levy's method, for a single-input-single-output (SISO) system was based upon expressing the TF in the form of frequency-dependent numerator $A(j\omega)$ and denominator $B(j\omega)$ polynomials as $H(j\omega) = B(j\omega)/A(j\omega)$ where ω is any frequency within the frequency range of interest in the specific problem. The experimental TF $\hat{H}(j\omega)$ is obtained from input/output measured data for the studied system. Thereafter, Levy (1959) considered the difference between the experimental and theoretical TFs as the error $e(j\omega) = B(j\omega)/A(j\omega) - \hat{H}(j\omega)$. The error formula was modified to a simpler form $\hat{e}(j\omega) = B(j\omega) - A(j\omega)\hat{H}(j\omega)$. Finally, by differentiating the norm of the simplified error evaluated at known frequencies with respect to the unknown coefficients of the polynomials $B(j\omega)$ and $A(j\omega)$, a number of equations (equivalent to the number of the unknown coefficients), are obtained. By solving these equations, the coefficients of $B(j\omega)$ and $A(j\omega)$ are obtained.

2.3.2 Time Domain Techniques

Time domain methods as well became quite popular later in the last century especially with the great advance in the computer systems industry (Juang, 1994). Many time domain identification techniques are explained thoroughly in Ljung (1999). Some examples of time domain identification techniques are ARX, ARMA, ARMAX, ERA, recursive least squares, etc. Also, Beck *et al.* (1994a) presented a methodology for determination of modal characteristics of structures from its measured ambient vibrations at several instrumented locations, an extension

of the MODE-ID algorithm that uses a Bayesian probability framework to build a linear model based on a classical normal modes approach (Beck, 1978; Beck, 1990).

2.3.3 ERA and Subspace Identification Techniques

One example of non-parametric time-domain methods is given by Juang and Pappa (1985), which proposed a method called the Eigensystem Realization Algorithm (ERA) for modal identification from measured responses. This method uses a singular-value decomposition to derive the basic formulation for a minimum-order realization, which is an extended version of the Ho-Kalman algorithm (Ho and Kalman, 1965). First, a block Hankel matrix is obtained by arranging the pulse response data into the blocks of the Hankel matrix. By examining the singular values of the Hankel matrix, the order of the system is determined. A minimum-order realization (**A**, **B**, and **C** state-space matrices) is constructed using a shifted block Hankel matrix. By finding the eigensolution of the realized state matrix, modal damping rates and frequencies may be obtained. The method then evaluates coherence and co-linearity accuracy parameters to separate system modes from noise modes. Based on these accuracy parameters, the system model is determined and the Hankel matrix based on identified state space matrices is reconstructed and compared with the measurement data.

Some modifications were later considered to improve the ERA method. Juang *et al.* (1988) introduced a modification to ERA algorithm, using response data correlations (ERA/DC) rather than the pulse response values in the formulation of the Hankel matrix. The ERA/DC modified method was found to reduce measurement noise bias without model over-specification. However, when over-specification is permitted and singular value decomposition is used to obtain a minimum order realization, both old and modified methods give equally good results for the data used.

Other subspace techniques have also been were also introduced and studied. Quek *et al*. (1999) introduced the Eigen-space Structural Identification technique for tall buildings subjected to stationary ambient excitations and based on the forward innovation model of the Kalman filter sequence. The method used QR decomposition and Quotient Singular Value Decomposition (QSVD) techniques, which are substituted into a least-square formulation to obtain a non-unique solution. Luş *et al*. (1999) presented an algorithm, based on the ERA and Observer/Kalman filter Identification (OKID) approaches, that uses earthquake-induced ground accelerations and structural vibrations as input/output data sets for identification purposes.

2.3.4 Structural Model Parameter Identification

Having accurate and updated information about the condition of structures, that may suffer hazardous shaking or loading, is crucial. This would save many lives as well as a lot of money. Accordingly, identifying the structural model parameters such as stiffness and damping is done to predict the behavior of structures under expected future loadings. Significant research effort, therefore, has been directed to find methods to identify these parameters. Some methods, such as that by Takewaki *et al.* (2000), have studied the stiffness-damping simultaneous identification of building structures using limited earthquake records with higher intensity level. Other research has been based on probabilistic methods related to Bayesian theory, such as Vanik *et al*. (2000) and Katafygiotis and Yuen (2001).

The focus of model parameter identification to achieve SHM is usually on local loss of stiffness as a proxy for local damage (Capecchi and Vestroni, 1999; Caicedo *et al.*, 2001; Elmasry and Johnson, 2002; Beck *et al.*, 1994b, 2001). To achieve that, some research has sought to identify relationships between change in the modal characteristics and changes in

structural properties such as mass, stiffness, and damping. For example Bayesian methodologies have been used for identifying the loss of structural stiffness, such as in Beck *et al.* (1994b, 2001). Bayes' theorem is invoked to develop a probability density function (PDF) for the model stiffness parameters conditioned on modal data and the chosen class of models. The latter method estimates the natural frequencies, damping ratios, and mode shape components of a linear model with classical normal modes that best fits the measured data in a least squares sense. Then the parameters of the structural model are determined from the computed modal data. The critical assumption is that the change in the structural model implies changes in the parts of the real structure. As a first step, changes in the values of the modal parameters are identified and then as a second step the corresponding loss of stiffness within the structure is identified.

In other previous research work focusing on identifying these model parameters, ambient vibration, such as ambient wind measurements, is used for excitation. Béliveau and Chater (1984) outlined a procedure to estimate parameters based on relatively simple ambient wind measurements of story accelerations reduced to resonant frequencies, and corresponding mode shapes. Also, several other research studies have considered ambient vibration for identification of stiffness parameters and, in turn, stiffness loss, such as Beck *et al*. (1994, 2001), and Caicedo *et al*. (2001). Ray and Tian (1999) introduced a method intended for smart structures embodying self-actuation and self-sensing capabilities. The method enhances modal frequency sensitivity to damage using feedback control.

2.4 Variable Stiffness/Damping Devices

"Smart" variable stiffness/damping devices (VSDDs), such as semiactive dampers and controllable stiffness devices, are controllable passive devices that potentially offer the reliability of passive devices, yet maintain the versatility and adaptability of fully active systems (Dyke *et al*., 1996). These devices have received significant study for mitigating various types of natural hazards for many types of civil structures (Spencer and Sain, 1997; Symans and Constantinou, 1999), and are useful for improving SHM.

2.4.1 Passive, Active and Semiactive Devices

Control devices for civil structures can be divided into four classes passive, active, semiactive and hybrid. Passive devices, generally, are those that have fixed properties and require no energy to function. In contrast, the controllable forces generated by active devices are induced directly by energy (electrical or otherwise) put into the device. Between passive and active are semiactive devices that are passive devices with properties that are controllable by application of a small amount of energy. Hybrid devices are combinations of the other three classes. Each of these is discussed briefly in the following paragraphs, with greater detail on semiactive devices.

Passive devices, such as visco-elastic dampers, viscous fluid dampers, friction dampers, metallic dampers, tuned mass dampers, and tuned liquid dampers can partially absorb structural vibration energy and reduce response of the structure (Soong and Dargush, 1997). These passive devices are relatively simple and easily replaced. However, the effectiveness of passive devices is always limited due to the narrow frequency ranges in which they tend to be effective, the dependence of their force only on local information, and their inability to be modified if goals (or design codes) change.

Active control devices, including active mass dampers and active tendon systems, can reduce structural response more effectively than passive devices because feedback and/or feed-

forward control systems are used (Housner *et al*., 1997). However, large power requirements during strong earthquakes and other hazards hamper their implementation in practice. Further, active devices have the ability to inject dynamic energy into the structural system; if done improperly, this energy has the potential to cause further damage to the structure. In particular, this can occur when the assumptions used to design the control algorithm are incorrect or do not have a proper characterization of the structural dynamics.

In contrast, "smart" devices are controllable passive devices that require small amounts of power to control certain passive behavior. Moreover, these devices cannot add energy to the structural/mechanical system; rather, they may only (temporarily) store and dissipate energy. Furthermore, they offer highly reliable operation at a modest cost and can be viewed as fail-safe in that they default to passive devices should the control hardware malfunction (Dyke *et al*., 1996).

2.4.2 Types of Semiactive Devices

Different types of semiactive devices have been developed recently. One type of is the semiactive damper, such as variable-orifice dampers, controllable fluid dampers, and controllable friction devices. Variable-orifice dampers use an electromechanical variable orifice to alter the resistance to flow in a conventional hydraulic fluid. Controllable fluid dampers are passive hydraulic dampers containing a fluid, such as magnetorheological (MR) or electrorheological (ER) fluid, with controllable yield stress (Spencer *et al*., 1997). Another type of semiactive device is a semiactive stiffness device such those developed by Kobori and Takahashi (1993), Patten *et al*. (1999) and Yang *et al*. (1996). They are on-off hydraulic devices capable of providing mainly variable damping and limited variable stiffness capability. Nagrarajaiah and Ma (1996) introduced a variable stiffness device that consists of four sets of spring elements and telescoping tube elements. Varying the position of the springs with a servomotor produces the continuously-variable stiffness.

Controllable fluid dampers use fluids with properties that can be modified by some outside influence. MR or ER fluids change their properties in the presence of a magnetic or electric field, respectively. These fluids were originally developed in the 1940s (Rabinow, 1948; Winslow, 1949), but few applications were foreseen at that time. While ER fluids showed early promise for civil applications (see, *e.g.*, Ehrgott and Masri, 1992), most of the attention of the civil structural control community has shifted to using MR fluids due to their insensitivity to impurities, relatively constant behavior over a wide range of operating temperatures, and the low voltage required to activate them (Spencer *et al.*, 1997). MR dampers typically consist of a hydraulic cylinder containing micron-sized magnetically polarizable particles suspended within a fluid. In the presence of magnetic field, the particles polarize and form particle chains that resist fluid flow. By varying the magnetic field, the mechanical behavior of an MR damper can be modulated. Since MR fluids can be changed from a viscous fluid to a yielding semisolid within milliseconds and the resulting damping force can be considerably large with a low-power requirement, MR dampers are applicable to large civil engineering structures.

2.4.3 Applications of Semiactive Control to Civil Structures

The idea of incorporating variable stiffness/damping devices in civil structures is not new. These devices have been extensively researched for base isolation of structures and other structural control applications, particularly in the last decade. Some researchers have investigated MR dampers for control of seismic response such as Dyke *et al*. (1996), Spencer *et al*. (1997, 1998) and Yang *et al.* (2002). ER dampers were studied for seismic response control by Ehrgott

and Masri (1992), Gavin *et al*. (1996a,b), Makris *et al*. (1996), and others. Dyke *et al*. (1996) proposed a clipped-optimal force control algorithm with acceleration feedback and obtained excellent results when this algorithm was applied to control a seismically excited three story scaled building model. Ribakov and Gluck (1999) investigated the effectiveness of ER dampers in mitigating seismic response of frame structures. They used an optimal linear passive control strategy to determine the viscous constant of the ER damper and then use active control strategy to determine control forces. Through numerical simulation they found that ER dampers could reduce the peak displacement response of a seven-story frame structure up to 65 per cent without increases in base shear forces and accelerations. In Xu *et al*. (2000), the force-displacement relationship of an MR damper or an ER damper, based on a parallel-plate model, is first extended to include the stiffness of chevron brace supporting the smart damper. An extensive parameter study is performed in terms of the maximum yield shear stress and the Newtonian viscosity of the fluid, the brace stiffness, and the earthquake intensity. VSDDs are also studied for damping of stay cables in suspended bridges. Johnson *et al*. (2003) investigated the potential of improving the damping to these cables through the use of semiactive damping devices. The response of the cables with a semiactive damper is found to be reduced dramatically compared to the optimal passive linear viscous damper for typical damper configurations, thus demonstrating the efficacy of a semiactive damper for absorbing cable-vibratory damage. Varadarajan and Nagrarajaiah (2000) introduce the use of semiactive variable stiffness tuned mass damper to control the response of tall buildings excited by wind. The results from the latter paper indicate that using the semiactive variable stiffness tuned mass damper is able to reduce the response similar to using an active tuned mass damper.

2.4.4 Experimental and Full Scale Studies Using Semiactive Devices

Since theoretical VSDD research has shown significant promise, researchers have progressed to experimental work to apply semiactive control in real world applications. Symans and Constantinou (1997) describe shaking table tests of a multi-story scale-model building structure subjected to seismic excitation and controlled by a semiactive fluid damper control system. The semiactive dampers were installed in the lateral bracing of the structure and the mechanical properties of the dampers were modified according to control algorithms that utilized the measured response of the structure.

Patten *et al*. (1999) reported the first successful full scale demonstration of semiactive control technology, installing an Intelligent Stiffener for Bridges (ISB) on an in-service bridge on interstate I-35. The ISB consists of an otherwise generic stiffener, retrofitted to a bridge, that is equipped with an adjustable hydraulic link used to regulate the amount of stiffness (and damping) provided by the stiffener as vehicles pass over the bridge. The ISB acts much like a muscle, sometimes flexing, and other times remaining relaxed. A 12-volt automobile battery energizes it. The performance of the installed ISB system was assessed via experimental results (see Fig. 6). The results indicate that the ISB system can add decades of service life to an existing bridge.

The Kajima Corporation has developed a semiactive hydraulic damper (SHD) and installed it in an actual building (Kurata *et al*., 2000). This was the first application of a semiactive seismic building control system that continuously changes the device damping coefficient. A forced vibration test was carried out by an exciter with a maximum force of 100 kN to investigate the building vibration characteristics and to determine the control system performance. As a result, the primary resonance frequency and the damping ratio of a building (without semiactive hydraulic dampers) decreased as the exciting force increased due to the influence of non-linear members such as plain concrete curtain walls. After the eight semiactive hydraulic dampers were installed in the building, the control system performance was identified by a response control test for steady-state vibration. The elements that composed the semiactive damper system demonstrated the specified performance and the whole system operated successfully, considerably reducing the displacements at the roof of the structure.

To prove the scalability of MR fluid technology to devices of size appropriate for civil engineering applications, Yang *et al.* (2002) study a MR fluid damper with a nominal maximum damping force of 200 kN (20 tons). For design purposes, two quasi-static models, an axisymmetric and a parallel-plate model, are derived for the force-velocity relationship of the MR damper, and both models give results that match closely match the experimental data.

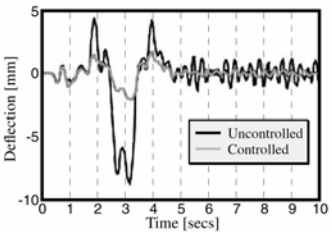

Figure 6. ISB vibration absorber on I-35 bridge (Patten *et al*., 1999)

3.0 PROJECT OBJECTIVE AND SUMMARY

The core of this research project has been to investigate whether and how variable stiffness and damping devices can be effectively used to identify local damage in bridge structures. A complete and conclusive answer to this question is beyond the scope of a one-year project, but it guides the direction of the ongoing research. This study is based on simulation of bridge motion due to ambient excitation. Using one or more variable stiffness and damping devices (VSDDs) to modify the response, structural parameters are estimated. The critical assumption is that the change in the structural model implies changes in the parts of the real structure. The focus is usually on local loss of stiffness as a proxy for local damage. The damage in this study is evaluated in terms of the loss of stiffness within a structural model, found by comparing the structural model parameters before and after damage occurrence given some input/output data.

One fundamental goal is to determine the best VSDD actions — whether adding damping or stiffness — to precisely and robustly locate and identify bridge damage. Several VSDD behaviors, such as variable stiffness mode and variable damping mode are considered. To reflect the generality of the approach of using VSDDs in SHM, this study includes bridge and building structures as well. Bridge and shear building model behaviors are assumed locally linear before damage and after damage. Some simple models of bridge dynamics are given herein to be used in simulation. The system models necessary for this study are *control-oriented* dynamic models — *i.e.*, low-order models that still capture the salient dynamic characteristics of a real bridge (or frame structure), particularly in the locations of the controllable devices and sensors, and across the frequency ranges driven by the excitation.

After the development of control-oriented models, the next step involves incorporating models of variable stiffness and damping devices into the dynamic bridge model and/or shear building model systems. Ideal stiffness devices with multiple discrete stiffness settings are used. A least-squares identification method of the related transfer functions is used to identify structural characteristics such as stiffness and damping or their ratios to the corresponding masses. The responses are simulated for the combined bridge/VSDD dynamic model and shear building models. By using the various permutations of stiffness device settings, multiple signatures are obtained that help better identify the structural parameters. Then, controllable damping devices are tested whether they can provide better information about structural model properties.

The method used herein to identify the structure model parameters is based on a least-squares error convergence technique. The error is expressed as the difference between the measured transfer functions (from the external excitation to the measured responses) and their corresponding polynomial parametric forms. In order to obtain the required structural parameters, the relationships between the structural model parameters and the polynomial coefficients are obtained. The problem is modeled as a single-input multi-output system (SIMO). One simplification that is discussed in the literature (Levy, 1959) is used to overcome the complexity of the direct transfer function polynomial identification. However, this simplification, denoted the "Least Squares Numerator Method," is hsown to lead to significant bias in parameter estimates due to unwanted effects of sensor noise. Consequently, an iterative method is proposed that approximates the more direct exact method. The proposed method is called the "Iterative Least-Squares Numerator Method." These methods are then applied to

conventional frequency domain structural identification, assuming no VSDD, and with one or more VSDDs with several distinct stiffness settings.

It is shown that, using the parametric frequency-domain least-squares approach with the proposed modified transfer function error and a known starting guess, the VSDD approach gives mean parameter estimate similar to that with a conventional structure but with rather smaller error (*i.e.*, smaller variance).

4.0 PARAMETRIC FREQUENCY DOMAIN IDENTIFICATION WITH VSDDS

4.1 Least-Squares Numerator Method (LSN)

One method of identifying parameters of a dynamical system is by representing transfer functions (TFs) in the frequency domain as ratios of polynomials. The transfer functions generally are defined by the ratio between the output and input signals. For example, consider a linear structural model of the form:

$$\mathbf{M}\ddot{\mathbf{x}} + \mathbf{C}_{\mathrm{d}}\dot{\mathbf{x}} + \mathbf{K}\mathbf{x} = \mathbf{b}f\ , \quad \mathbf{y} = \mathbf{C}_1\mathbf{x} + \mathbf{C}_2\dot{\mathbf{x}} + \mathbf{d}f + \mathbf{v} \tag{1}$$

where **M**, **K**, and $\mathbf{C}_{\mathrm{d}}$ are the mass, stiffness and damping matrices of the system, and $\mathbf{C}_1$, $\mathbf{C}_2$, and **d** are the output influence matrices for the displacement, velocity and the external force *f*. For simplicity of the method developed herein, the input force is assumed to be a single scalar force. Similarly, one can write the model in state-space form

$$\dot{\mathbf{q}} = \tilde{\mathbf{A}}\mathbf{q} + \tilde{\mathbf{B}}f\ , \qquad \mathbf{y} = \mathbf{C}\mathbf{q} + \mathbf{D}f + \mathbf{v} \tag{2}$$

where $\mathbf{q} = \begin{bmatrix}\mathbf{x}^{\mathrm{T}} & \dot{\mathbf{x}}^{\mathrm{T}}\end{bmatrix}^{\mathrm{T}}$ is the state vector, $\tilde{\mathbf{A}}$ is the system state matrix which is dependent on the mass, damping, and stiffness matrices, $\tilde{\mathbf{B}}$ is the input influence matrix, **C** is the output influence matrix for the state vector **q,** and **D** is the direct transmission matrix. In both equations, *f* is an excitation force, and **y** is an $m \times 1$ vector of measured responses corrupted by $m \times 1$ sensor noise vector **v**.

Thus, the system can be represented by the $m \times 1$ transfer function matrix **H**($j\omega$). Each element of **H**($j\omega$) can be expressed as the ratio of numerator and denominator polynomials at a certain frequency with coefficients depending on matrices in Eqs. (1) or (2). It is important to state that for many structural systems, the denominator polynomial is the same for all transfer functions from the same input. Therefore, identifying the denominator polynomial is crucial in defining the system dynamics. The transfer function vector from a single input to the outputs can consequently be written in polynomial ratio form as:

$$\mathbf{H}(j\omega) = \mathbf{B}(j\omega) / A(j\omega) \tag{3}$$

where **B**($j\omega$) and $A(j\omega)$ are the numerator and denominator polynomials, which may be expanded $B_r(j\omega) = b^r_{n_B-1}(j\omega)^{n_B-1} b^r_{n_B-2}(j\omega)^{n_B-2} + \ldots + b^r_0$ and $A(j\omega) = a_{n_A}(j\omega)^{n_A} + a_{n_A-1}(j\omega)^{n_A-1} + \ldots + a_0$, where the *b*'s and *a*'s are real coefficients.

Assuming that the transfer function has been determined experimentally through standard procedures from measured input and output data (Bendat and Piersol, 2000), the experimental transfer function matrix, expressed as

$$\hat{\mathbf{H}}(j\omega_i)\ , \ i=1, 2, \ldots, n_\omega \tag{4}$$

is known at various discrete frequency points. Therefore, the difference between the estimated theoretical transfer function **H**($j\omega$) and the actual experimental one $\hat{\mathbf{H}}(j\omega)$ represent the error equation which is then used in the identification process of the parameters.

Parametric frequency-domain methods to match such theoretical and measured transfer functions date back to the work of Levy (1959) who parameterized a continuous-time TF by the coefficients of numerator and denominator polynomials. One approach to this problem is to

follow Levy's procedure in determining the polynomial coefficients and then, as a subsequent step, estimate structural parameters such as mass, stiffness and damping coefficients. The latter could be through an intermediate step of first identifying modal characteristics such as modal frequency, damping ratio and mode shapes. In this study, however, the parameterization method is chosen to be through the structural parameters directly without calculating the coefficients of the polynomials as an intermediate step.

For a structure with one or more variable stiffness and/or damping devices, the properties of which are determined through a local control system, some of the coefficients in the transfer function polynomials may be adjusted through changing the VSDD control algorithms. Thus, it is convenient to introduce notation to explicitly state that the transfer function polynomials are functions of unknown structural parameters, denoted by the $n \times 1$ vector $\boldsymbol{\theta}$, which is to be estimated, and of known controllable structural parameters, denoted by the vector $\boldsymbol{\kappa}$. The transfer function expression is thus modified to be:

$$\mathbf{H}(j\omega) = \mathbf{B}(j\omega, \boldsymbol{\theta}, \boldsymbol{\kappa}) / A(j\omega, \boldsymbol{\theta}, \boldsymbol{\kappa}) \tag{5}$$

For a given structural model, the A and $\mathbf{B}$ polynomials are specific known functions of their parameters. Substituting the measured TF in place of the exact TF leaves a residual error $\mathbf{e}$ that may be defined by

$$\mathbf{e}(j\omega_i, \boldsymbol{\theta}, \boldsymbol{\kappa}) = \frac{\mathbf{B}(j\omega_i, \boldsymbol{\theta}, \boldsymbol{\kappa}) - A(j\omega_i, \boldsymbol{\theta}, \boldsymbol{\kappa})\hat{\mathbf{H}}(j\omega_i, \boldsymbol{\kappa})}{A(j\omega_i, \boldsymbol{\theta}, \boldsymbol{\kappa})} \tag{6}$$

A conventional least-squares approach may be adopted to solve this problem, forming a global square error

$$\boldsymbol{\Delta}^2(\boldsymbol{\theta}) = \sum_i \mathbf{e}^*(j\omega_i, \boldsymbol{\theta}, \boldsymbol{\kappa}) \cdot \mathbf{e}(j\omega_i, \boldsymbol{\theta}, \boldsymbol{\kappa}) \tag{7}$$

where $(\cdot)^*$ denotes complex conjugate transpose. The optimal choice of the unknown parameters is found by minimizing the square error — *i.e.*, take the derivatives of the square error Eq. (7) with respect to the elements of unknown vector $\boldsymbol{\theta}$, set them equal to zero, and solve the resulting (generally nonlinear) equations. However, if there are known controllable structural parameters in a structure with multiple configurations — which is the case when using VSDDs, for example — the square error equation can be augmented by using several combinations of known controllable structural parameters

$$\boldsymbol{\Delta}^2(\boldsymbol{\theta}) = \sum_k \sum_i \mathbf{e}^*(j\omega_i, \boldsymbol{\theta}, \boldsymbol{\kappa}_k) \cdot \mathbf{e}(j\omega_i, \boldsymbol{\theta}, \boldsymbol{\kappa}_k) \tag{8}$$

where the symbol $\boldsymbol{\kappa}_k$ denotes multiple distinct sets of parametric changes to the structure. The error is, then, minimized simultaneously for all configurations.

Because the residual error $\mathbf{e}$ in Eq. (6) is a ratio of polynomials, the square error in Eq. (8) is an extremely complex function of the unknown parameters $\boldsymbol{\theta}$. One simplification, which has been suggested and used in various studies in the literature, is to recognize that the denominator of Eq. (6) is nonzero for systems with damping, so minimizing the error in the numerator may prove sufficient (*e.g.*, Levy, 1959). In other words, minimize the sum of the squares of:

$$\tilde{\mathbf{e}}(j\omega_i, \boldsymbol{\theta}, \boldsymbol{\kappa}_k) = \mathbf{B}(j\omega_i, \boldsymbol{\theta}, \boldsymbol{\kappa}_k) - A(j\omega_i, \boldsymbol{\theta}, \boldsymbol{\kappa})\hat{\mathbf{H}}(j\omega_i, \boldsymbol{\kappa}_k) \tag{9}$$

which is, herein, denoted the *least-squares numerator* (LSN) method.

4.2 Iterative-Least Squares Numerator Method (ILSN)

It may be shown that the alternate error measure in the LSN method, while simpler to solve, can be susceptible to strong bias from sensor noise in frequency ranges where $A(j\omega_i, \boldsymbol{\theta}, \boldsymbol{\kappa})$ is large (*i.e.*, often the case where $\mathbf{H}(j\omega)$ is small). To avoid this bias, and to avoid the difficulty in solving the least-squares problem for the standard error measure $\mathbf{e}$, an *iterative* method, described as follows, is adopted here using an approximation to the denominator in Eq. (6).

Assume that iteration l begins with a starting approximation $\hat{\boldsymbol{\theta}}_{l-1}$ to the unknown parameter vector $\boldsymbol{\theta}$; then, the denominator of Eq. (6) is estimated based on the vector $\hat{\boldsymbol{\theta}}_{l-1}$ of estimated parameters and is no longer a function of these unknowns, but only in the frequency and the multiple distinct sets of parametric changes to the structure

$$\hat{A}_l(j\omega_i, \boldsymbol{\kappa}_\kappa) \equiv \hat{A}(j\omega_i, \hat{\boldsymbol{\theta}}_{l-1}, \boldsymbol{\kappa}_\kappa) \tag{10}$$

and the error is, thus, formed as

$$\hat{\mathbf{e}}_l(j\omega_i, \boldsymbol{\theta}, \boldsymbol{\kappa}_\kappa) = \frac{\mathbf{B}(j\omega_i, \boldsymbol{\theta}, \boldsymbol{\kappa}_\kappa) - A(j\omega_i, \boldsymbol{\theta}, \boldsymbol{\kappa}_\kappa)\hat{\mathbf{H}}(j\omega_i, \boldsymbol{\kappa}_\kappa)}{\hat{A}_l(j\omega_i, \boldsymbol{\kappa}_\kappa)} \tag{11}$$

and the squared error takes the form:

$$\boldsymbol{\Delta}_l{}^2(\boldsymbol{\theta}) = \sum_k \sum_i \hat{\mathbf{e}}_l{}^*(j\omega_i, \boldsymbol{\theta}, \boldsymbol{\kappa}_\kappa) \cdot \hat{\mathbf{e}}_l(j\omega_i, \boldsymbol{\theta}, \boldsymbol{\kappa}_\kappa) \tag{12}$$

Minimizing the sum of the square error in Eq. (12) will result in an updated estimate $\hat{\boldsymbol{\theta}}_l$ to the unknown parameter vector $\boldsymbol{\theta}$. The iterations continue until the relative differences between $\hat{\boldsymbol{\theta}}_{l-1}$ elements and the corresponding elements of $\hat{\boldsymbol{\theta}}_l$ are all below some threshold. (Absolute or relative norms of the difference could also be used.) A maximum number of iterations may also be set to stop the algorithm in the case that the iterative method does not converge (though this termination criterion was not required in this study as convergence always occurred within a limited number of iterations).

Whichever method is used to estimate the unknown parameter vector $\boldsymbol{\theta}$, the use of multiple structural configurations, denoted by the different values of known parameters $\boldsymbol{\kappa}_k$, provided by VSDDs in a structure, can generate more accurate estimates of $\boldsymbol{\theta}$ than can be found with a comparable amount of data in a conventional structure with a fixed $\boldsymbol{\kappa}$. This is demonstrated for some examples in the following section.

4.3 Illustrative Examples

The least-squares identification with VSDDs may be applied to various types of structures. In this study, both building and bridge models are considered.

4.3.1 Two Degree-of-Freedom Shear Building Model

Consider the two degree-of-freedom (2DOF) shear building structure model shown in Fig. 7. The structure is subject to ambient excitation from the ground. Absolute accelerations measurements at the ground, $\ddot{x}_g$, and of the two floors, $(\ddot{x}_1 + \ddot{x}_g)$ and $(\ddot{x}_2 + \ddot{x}_g)$, are used to generate a 2×1 experimental transfer function at n_ω distinct frequency values. (Note that x_i herein denotes the displacement of the i^{th} floor relative to the ground.) Let the unknown parameter vector be given by:

$$\boldsymbol{\theta} = \left[\frac{k_1}{m_1} \quad \frac{k_2}{m_2} \quad \frac{c_1}{m_1} \quad \frac{c_2}{m_2} \quad \frac{m_2}{m_1} \right]^{\mathrm{T}} \tag{13}$$

A VSDD that can provide a number of distinct stiffness levels is located in the first story of the structure. The VSDD is installed in the lateral bracing of the structure and the mechanical properties of the dampers are modified according to control algorithms, which utilize the measured response of the structure. The device is considered ideal and semiactive; *i.e.*, it can generate the desired forces with no delay and with no actuator dynamics (Ramallo *et al*., 2000). Therefore the known controllable vector is related to the stiffness of a variable stiffness device

$$\boldsymbol{\kappa} = \kappa = k_{VSDD} / m_1 \tag{14}$$

or to the damping coefficient of a variable damping device

$$\boldsymbol{\kappa} = \kappa = c_{VSDD} / m_1 \tag{15}$$

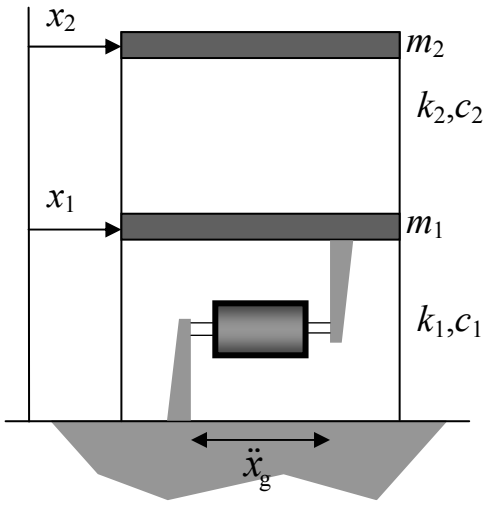

Figure 7. 2DOF shear building model

Then, the theoretical transfer function can be written in the polynomial form as:

$$\mathbf{H}(j\omega,\kappa) = \left[\frac{B_1(j\omega,\boldsymbol{\theta},\kappa)}{A(j\omega,\boldsymbol{\theta},\kappa)} \quad \frac{B_2(j\omega,\boldsymbol{\theta},\kappa)}{A(j\omega,\boldsymbol{\theta},\kappa)} \right]^{\mathrm{T}} \tag{16}$$

Note that the denominator polynomial $A(j\omega,\boldsymbol{\theta},\kappa)$ is the same for all transfer functions from the same input. The numerator and denominator polynomials can be expressed as:

$$\begin{aligned} A(s,\boldsymbol{\theta},\kappa) &= s^4 + [\theta_3+\theta_4+\theta_4\theta_5]s^3 + [\theta_1+\theta_2+\theta_2\theta_5+\theta_3\theta_4+\kappa]s^2 + [\theta_1\theta_4+\theta_2\theta_3+\kappa\theta_4]s + [\theta_1\theta_2+\kappa\theta_2] \\ B_1(s,\boldsymbol{\theta},\kappa) &= [\theta_3]s^3 + [\theta_1+\theta_3\theta_4+\kappa]s^2 + [\theta_1\theta_4+\theta_2\theta_3+\kappa\theta_4]s + [\theta_1\theta_2+\kappa\theta_2] \\ B_2(s,\boldsymbol{\theta},\kappa) &= [\theta_3\theta_4]s^2 + [\theta_1\theta_4+\theta_2\theta_3+\kappa\theta_4]s + [\theta_1\theta_2+\kappa\theta_2] \end{aligned} \tag{17}$$

The parameter identification methods discussed in the previous section can then be applied. The explicit reference to m_1 has dropped out of the transfer function polynomials; it will be assumed here that of all the parameters, only m_1 is known.

Different VSDD locations in the structure are studied in order to investigate the best way of using these VSDDs to improve SHM through better identification of the structural model parameters. Accordingly, this example is also solved considering a VSDD that can provide a number of distinct stiffness levels located in the second story of the structure and in both stories as well, as shown in Figs. 8 and 9. This will generally give an idea of how VSDD should be distributed in a structure for good SHM. In all cases, the VSDD is chosen to act as an ideal variable stiffness/damping device, with one of several discrete stiffness/damping values. Some examples from simulation are used to demonstrate the proposed method. This 2DOF model system identification was solved for the variable stiffness VSDD and for a conventional structure (no VSDD). In the simulations, each installed VSDD is assumed to provide additional stiffness at five discrete levels: 0%, 10%, 20%, 30% and 40% of the stiffness of the story at which it is located.

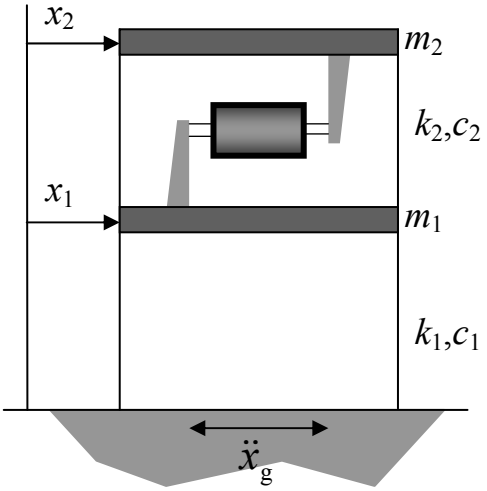

Figure 8. VSDD in 2nd story of 2DOF model

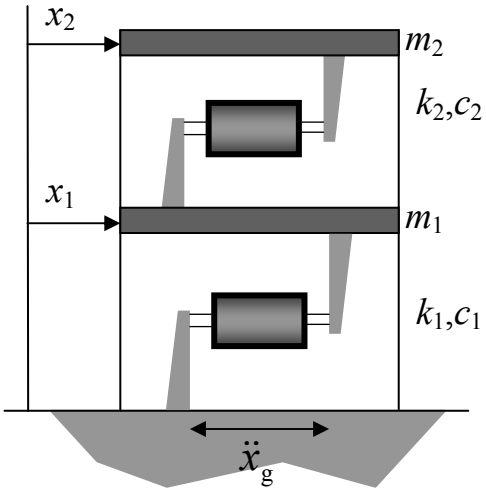

Figure 9. VSDDs in both stories of 2DOF model

4.3.2 Two Degree-of-Freedom Pier-Deck Bridge Model

Consider a bridge structure such as one shown in Fig. 10, which is a typical elevated highway bridge that consists of decks, bearings, and piers. The behavior of the bridge deck and piers, with a bearing between them, while complex, can be well approximated with the simple 2DOF model shown in Fig. 11*c*. This 2DOF model may be used to represent a passive system with rubber bearings if the girder is continuous with one pier and one bearing, or for several piers and bearings with identical properties. Also, this model can be used for VSDD systems if the devices are attached as shown in Fig. 12 and commanded to provide identical force levels. It is assumed in this problem that the pier mass m_1 is known.

Figure 10. General view during construction of high occupancy vehicle (HOV) lanes (ADOT, 2001)

The theoretical polynomial transfer function matrix $\mathbf{H}(j\omega,\kappa)$ is defined similarly to Eq. (16) where, here, $B_1(j\omega,\boldsymbol{\theta},\kappa)/A(j\omega,\boldsymbol{\theta},\kappa)$ is the transfer function between the ground acceleration and the absolute acceleration of the pier and $B_2(j\omega,\boldsymbol{\theta},\kappa)/A(j\omega,\boldsymbol{\theta},\kappa)$ is the transfer function between the ground acceleration and that of the bridge deck. The unknown parameter vector $\boldsymbol{\theta}$ is defined similar to Eq. (13) but k_1, is the stiffness of the pier and k_2 the stiffness of the deck. The vector of known parameters $\boldsymbol{\kappa}$ denotes the additional stiffness added through the VSDD connected between the pier and the deck. In the simulations, the installed VSDD is assumed to provide additional stiffness at five discrete levels: 0%, 10%, 20%, 30% and 40% of

the stiffness of the deck. A second, related example will use five similar discrete levels of VSDD damping instead of stiffness.

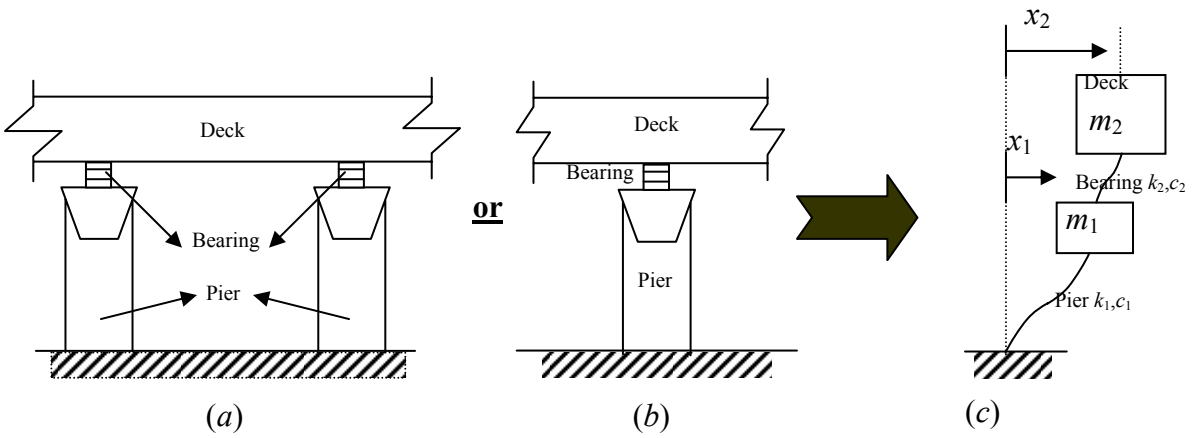

Figure 11. 2DOF bridge model

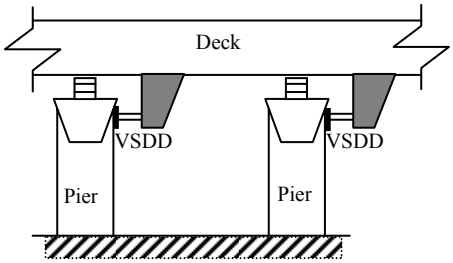

Figure 12. Placement of VSDDs in bridge

4.3.3 Six Degree-of-Freedom Shear Building Model

To demonstrate that these methods can be extended to more complex problems, a six degree-of-freedom shear building model is also studied. The shear building model is found to be a good representation for general problems that may exist in multi-story (or multi degree of freedom (MDOF) structures. This 6DOF model system identification was solved for the variable stiffness VSDD and the conventional structure (no VSDDs). In simulation, each installed VSDD is assumed to provide additional stiffness at four discrete levels: 0%, 10%, 20%, and 30% of the stiffness in the story at which it is located. The VSDD devices included in the structure are also considered ideal; *i.e.*, they can generate the desired forces with no delay and with no actuator dynamics. In this problem, the VSDDs are considered to be located in the first three stories only, as shown in Fig. 13, to make best use of VSDDs in the structure without escalating the expenditures too much.

It is important to note that applying the ILSN method for estimation of parameters in case of higher degrees of freedom (such as the 6DOF model) was very challenging in terms of RAM availability and computational speed. Some details about the numerical procedure to solve these difficulties are provided in Appendix A.

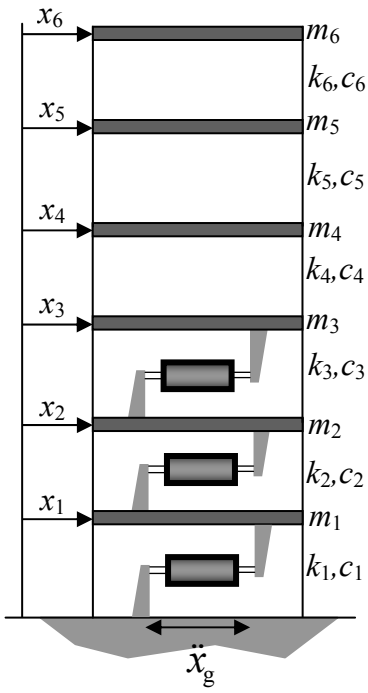

Figure 13. 6DOF model with VSDDs in first three stories

Here, masses are assumed a prior whereas the previous 2DOF model assumed knowledge only of the first mass. The unknown parameter vector $\boldsymbol{\theta}$ for the six degree-of-freedom model is, then, a set of unknown stiffness k_i and damping c_i coefficients as follows:

$$\boldsymbol{\theta}=[k_1 \;\; k_2 \;\; k_3 \;\; k_4 \;\; k_5 \;\; k_6 \;\; c_1 \;\; c_2 \;\; c_3 \;\; c_4 \;\; c_5 \;\; c_6]^{\mathrm{T}} \tag{18}$$

Finally, the solution for the parameters was done using the MATLAB® software and using the function `fsolve( )` for the solution of the non-linear equations in the unknown parameters $\boldsymbol{\theta}$.

4.4 NUMERICAL EXAMPLES AND ANALYSIS OF RESULTS

To demonstrate the benefits and the advantages of testing a structure with VSDDs configured in multiple settings, some numerical examples are considered.

4.4.1 Two Degree-of-Freedom Shear Building Model

First, a numerical example of the 2DOF structure is studied. For simplicity, the floor masses and story stiffnesses are taken to be unity in the numerical model. The story damping coefficients are set to 0.05, which results in 1.5% and 4.0% modal damping in the two modes, respectively. The single VSDD is assumed to provide additional stiffness in the story at which it is located with five discrete stiffness levels, corresponding to an additional 0%, 10%, 20%, 30% and 40% stiffness; *i.e.*, $\kappa_1 = 0.0$, $\kappa_2 = 0.1$, …, $\kappa_5 = 0.4$. The primary comparison reported here is the difference between:

- the *VSDD* approach, using five experimental transfer function matrices, one per VSDD stiffness level, and
- the *conventional structure* approach with $\kappa = 0.0$ — to make for a fair comparison using the same amount of data, the conventional approach uses a square error based on five separate experimental transfer functions.

The experimental transfer functions are generated in MATLAB by using the exact transfer functions plus the Fourier transform of a Gaussian pulse process that would be typical of band-limited Gaussian white sensor noise vector processes. The sensor noise used in generating the five experimental *VSDD* transfer functions is the same as those used for the *conventional structure* approach.

The number of evenly-spaced frequency points n_ω is 51. Figure 14 shows a comparison, in both linear and log scales, of the exact transfer function magnitudes that represents the true model with those of the experimental transfer function corrupted by noise for zero VSDD stiffness; this noise level provides a fairly challenging problem.

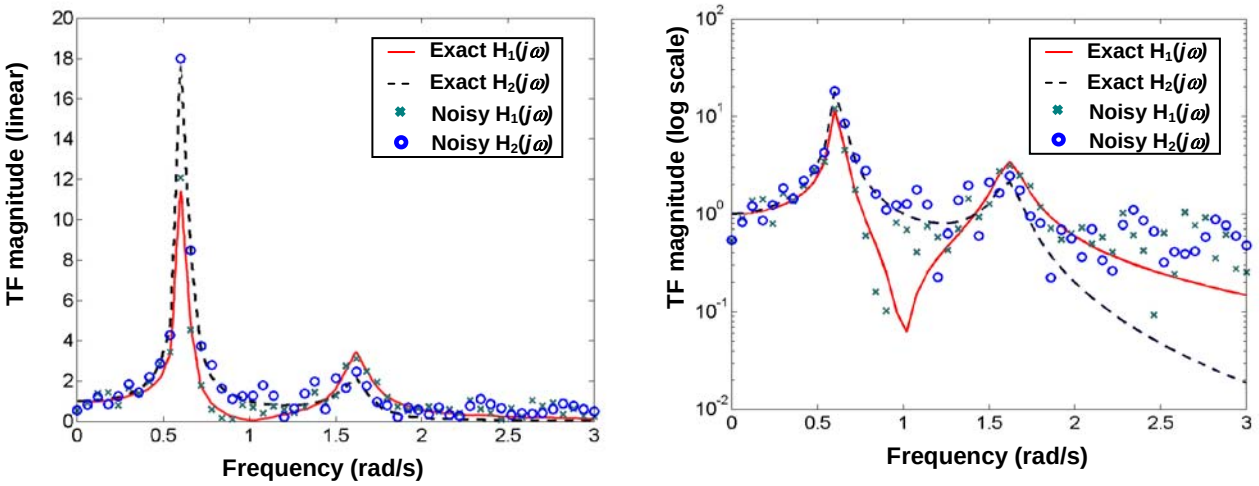

Figure 14. Exact and noisy TF magnitudes

Once the experimental transfer functions are generated, MATLAB® code employing the Symbolic Math Toolbox™ is used to determine the total square error symbolically. The result is then differentiated with respect to the unknown parameter vector $\boldsymbol{\theta}$, giving a number of equations that should equal zero. These equations, which are cubic polynomials in $\boldsymbol{\theta}$ for the parameterization in Eq. (13), are solved numerically using `fsolve()` function in the Optimization Toolbox™ with function tolerances and $\boldsymbol{\theta}$ solution tolerances both set to 10^{-5}. The iterative approach uses a relative tolerance of 10^{-4} (which must be met for all elements of the unknown parameter vector $\boldsymbol{\theta}$) as a termination criterion.

Least-Squares Numerator Method Results

First, the expected bias in the least-squares numerator method is verified by using the error definition in Eq. (9). The *VSDD* and *conventional structure* approaches are used to determine the unknown parameters. Each approach is performed 26 times, with 26 different seeds for generating the random noise, to see the distribution of error levels that may be expected with the least-squares numerator method. The initial $\boldsymbol{\theta}$ guess provided to the numerical equation solver is the exact value. Figure 15, which shows the error in the stiffness estimates for the 26 trials, demonstrates that both approaches give significant error in the estimates as well as a wide systematic bias. This bias is expected, as the denominator magnitude is quite large for higher frequency points as shown in Fig. 16, causing the noise to significantly skew the parameter estimates. Therefore, one can conclude that, as expected, this simplified technique cannot be adopted for fair comparison between the VSDD and *conventional structure* approaches because the results are not accurate.

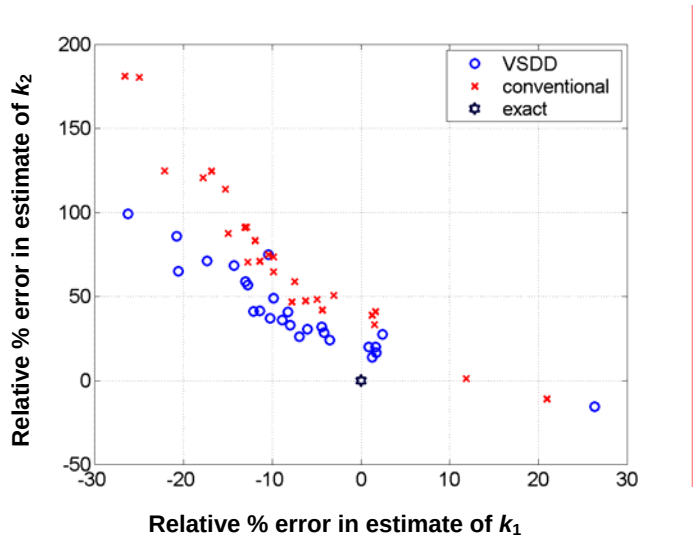

Figure 15. Stiffness estimate error levels with least-squares numerator method

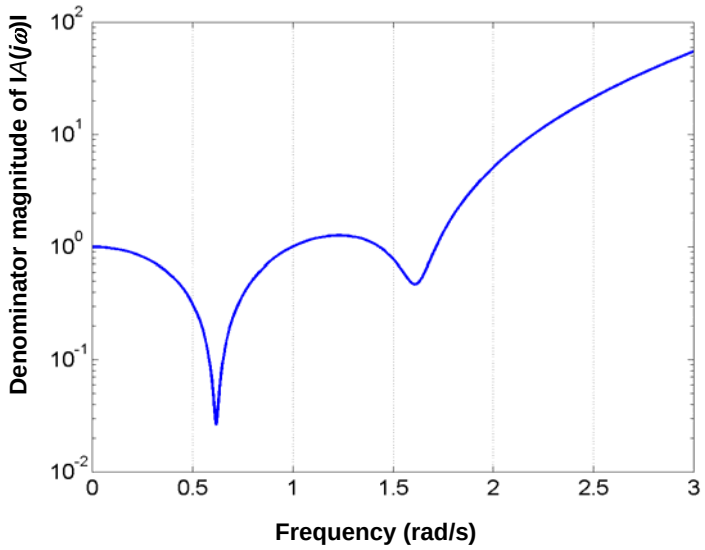

Figure 16. Denominator magnifies error at higher frequency with LSN method.

Results with the Iterative Method

The iterative approach gives significantly better results. Using the true parameter vector as an initial starting guess for the iterative procedure, the algorithm converges, generally in 3–5 iterations, to estimates that are fairly accurate — much better than the least-squares numerator method. Figure 17 shows the relative error in the estimates of the stories stiffness for the c*onventional structure* and *VSDD* approaches. Here, 100 separate estimates were computed (each with a different noise seed) to examine the variation due to sensor noise. The graph also shows approximate one-, two- and three-sigma (standard distribution) curves representing for the

two approaches. The curves were generated, assuming a Gaussian distribution, using the means and covariance matrix of the 100 estimates. The variation in estimates of first- and second-story stiffness using the *VSDD* approach are about half and two-thirds, respectively, of those using the *conventional structure* (without VSDDs).

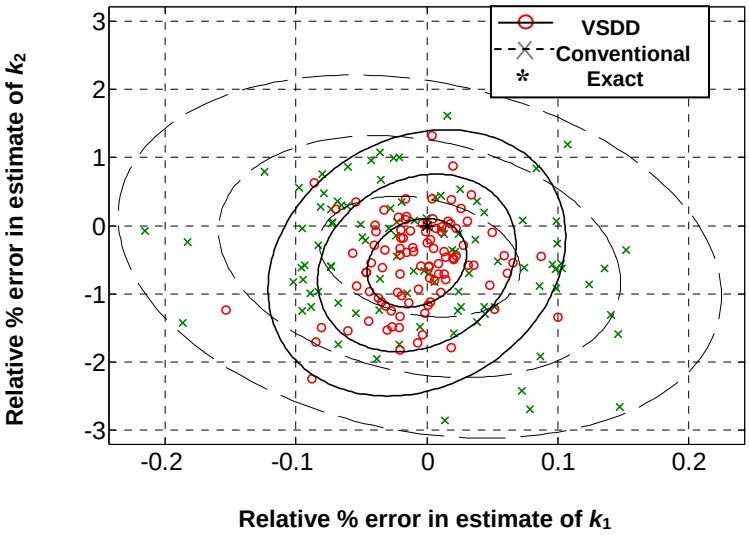

Figure 17. Stiffness estimate error levels for iterative method with exact start for 2DOF model with VSDD in 1st story only

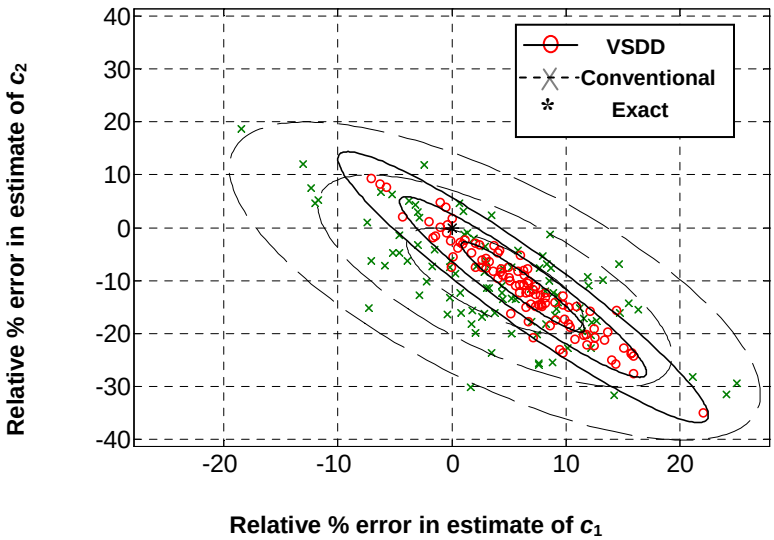

Figure 18. Damping estimate error levels for the iterative method with exact start for 2DOF model with VSDD in 1st story only

Damping estimates are, as expected, much less accurate for both approaches. Figure 18 shows the error variation in damping coefficient estimates using the ILSN method, and demonstrates that the *VSDD* approach has again generated a smaller variation as sensor noise changes. The relative error in this case is somewhat larger than that of the stiffness estimates, equals 22% using *VSDDs* and 27% for the conventional structure case in estimating the damping coefficient in the first floor c_1, and 36% and 40% for the estimation of the damping coefficient in the second floor c_2. This larger relative damping estimate error, for both *VSDD* and *conventional structure* approaches, compared to stiffness, is typical of most identification methods. Yet, it is clear that the *VSDD* approach, while not making vast improvements, shows some decrease in error compared to the *conventional* approach.

An initial guess that is biased, offset from the correct parameter vector by some amount, would be expected to give poorer estimates. This is indeed the case. Using an initial parameter vector that is 20% higher (in all components) than the exact values, 20 separate estimates were computed. Figure 19 shows that both approaches, as anticipated, are much less accurate in estimating the stories stiffness than with the exact initial guess. Here, the *VSDD* approach gives estimate means that are less biased than the *conventional structure* approach, though with slightly larger variation in the estimate of k_1. Again, this indicates that using VSDDs improved the stiffness estimates.

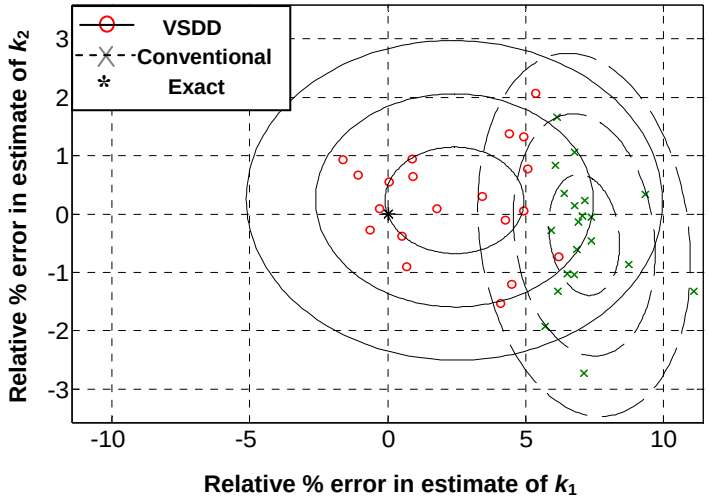

Figure 19. Stiffness estimate error levels for the iterative method with offset start for 2DOF model with VSDD in 1st story only

The computational effort to solve these problems symbolically was much higher than anticipated. To compute one estimate with the correct initial starting guess took approximately 15 minutes on a 600 MHz Pentium III computer. This is based on using the symbolic Math toolbox of MATLAB which is powered by MAPLE®. With an offset starting guess, more iterations were required, both in the iterative approach outlined above as well as within the numerical solver `fsolve( )`, requiring slightly longer to converge. The estimate means and coefficients of variation are shown for the two approaches in Table 1. The average number of iterations required for the MATLAB solver to converge are always less in case of *VSDD* approach than the *conventional structure* approach as shown in Table 1.

Table 1. Estimate Means and Coefficients-of-Variation for 2DOF Shear Building Model

Variables	exact	mean				coeff. of variation[%]			
		exact init. guess		*offset init. guess*		*exact init. guess*		*offset init. guess*	
		Conv. Struct.	VSDD	Conv. Struct.	VSDD	Conv. Struct.	VSDD	Conv. Struct.	VSDD
θ_1	1	0.9999	0.9999	1.0711	1.0241	0.0770	0.0390	1.1990	2.4560
θ_2	1	0.9972	0.9970	0.9337	0.9845	0.5310	0.3660	1.2620	1.8750
θ_3	0.05	0.0519	0.0531	0.0523	0.0521	7.4810	5.0920	6.2690	7.1560
θ_4	0.05	0.0450	0.0445	0.0477	0.0460	11.224	9.5930	9.2310	13.491
θ_5	1	0.9982	0.9975	1.0672	1.0183	0.3780	0.2950	1.1220	1.8370
k_1	1	0.9999	0.9999	1.0711	1.0241	0.0770	0.0390	1.1990	2.4560
k_2	1	0.9955	0.9945	0.9964	1.0023	0.8930	0.6570	1.0410	0.9100
c_1	0.05	0.0519	0.0531	0.0523	0.0521	7.4810	5.0920	6.2960	7.1560
c_2	0.05	0.0449	0.0444	0.0509	0.0469	11.163	9.6220	9.1460	14.165
m_2	1	0.9982	0.9975	1.0672	1.0183	0.3780	0.2950	1.1220	1.8370
		average no. of iterations	0	4.9800	4.0600	5.0500	4.8500		

VSDD in Second or Both Stories

To understand the effect of VSDD location(s) on the estimation, this 2DOF numerical example is modified to consider a VSDD in the second story. Trying to know the best location for VSDD within the structure, this numerical example is extended to consider the existence of VSDD in the second story, and in both stories. Again, comparison is made in each case to the *conventional approach* with no VSDDs located in the structure. The parametric frequency domain identification is applied and the results with a VSDD in the second story or one in each of the two stories are compared with those in *conventional structure* case.

From Fig. 20, it can be observed that the variation of the stiffness in the second story was clearly reduced, giving better identification of the second-story stiffness compared to a VSDD in the first story only. However, the variation in estimation of the first-story stiffness k_1 is larger with the second-story VSDD than with the *conventional* approach. Figure 21 shows that the damping estimation is still poor, as seen in the previous section. Yet, the VSDD still improves over the *conventional structure* approach.

Finally, two VSDDs are considered, one located in each story. Several simultaneous values of both VSDDs are considered. Each VSDD is controlled to exert an extra stiffness of 0%, 20%, 30%, and 40% each in its location. Five different profiles of simultaneous values of the exerted extra stiffness by both VSDDs are considered in the identification problem such that the values of additional stiffness are (0%,0%), (0%,40%), (20%,30%), (30%,20%) and (40%,0%) of the stiffness of each story, respectively. The results of the stiffness parameter identification problem are compared, similarly to the previous cases, to data from conventional structure simulations (so the amount of data is the same in both cases).

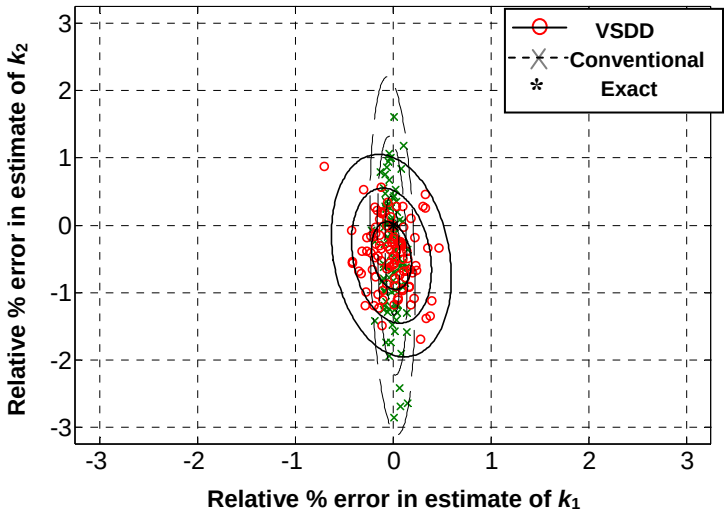

Figure 20. Stiffness error levels for the iterative method with exact start for 2DOF model with VSDD in 2nd story only

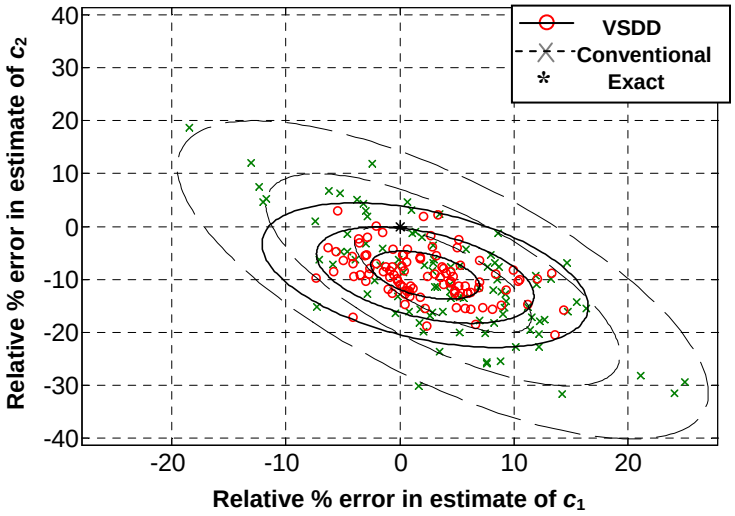

Figure 21. Damping error levels for the iterative method with exact start for 2DOF model with VSDD in 2nd story only

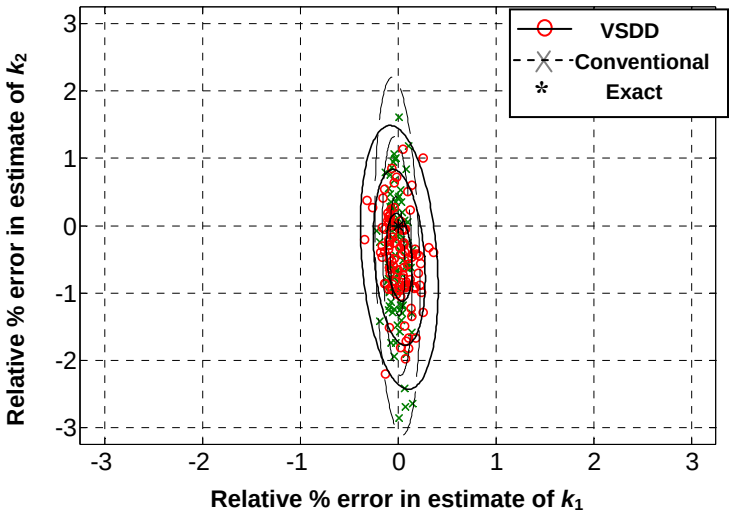

Figure 22. Stiffness error levels for the iterative method with exact start for 2DOF model with VSDD in both 1st and 2nd stories

The stiffness estimate results in Fig. 22 show that though the variation of the stiffness identification of the second story is clearly decreased and improved, the variation of the stiffness identification of the first story is still more than the conventional approach case. However, some improvement in the variation of the stiffness of the first story compared to the case of a VSDD in the second story can be noticed. As a result of that, it can be deduced that VSDDs may be most effective in identifying the stiffness of the stories or levels where they are located. However, multiple VSDD simultaneously may provide decreasing returns in a 2DOF structure, which may not be a fact for more complex structures. Comparing Figs. 18, 21 and 23, it is obvious that using a VSDD in each story simultaneously results in better identification of the damping coefficients of the first and second stories. The variation of the damping coefficients is reduced significantly and the means are more accurate.

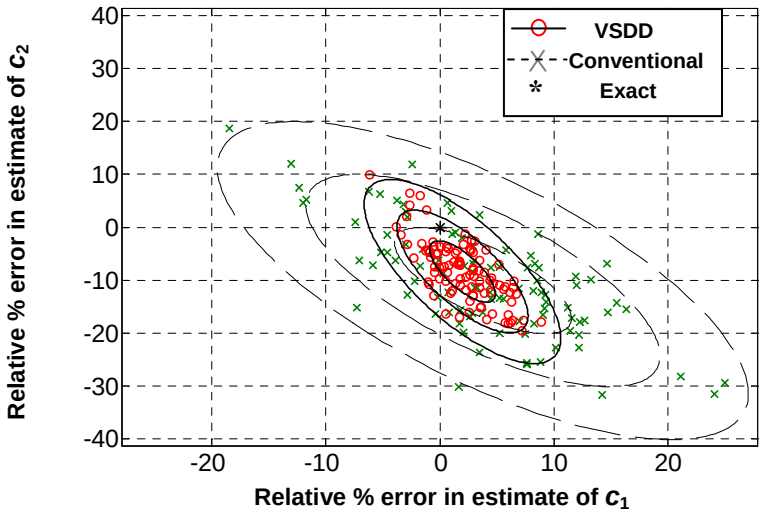

Figure 23. Damping error levels for the iterative method with exact start for 2DOF model with VSDD in both 1st and 2nd stories

Table 2. Range of 3σ Stiffness and Damping Estimate Relative Errors for 2DOF Shear Model

Initial guess	Case	k_1	k_2	c_1	c_2
Exact	Conventional structure	[–0.24%, 0.23%]	[–3.1%, 2.2%]	[–20%, 27%]	[–40%, 20%]
	VSDD in 1st story	[–0.13%, 0.11%]	[–2.4%, 1.4%]	[–10%, 23%]	[–22%, 5.0%]
	VSDD in 2nd story	[–0.70%, 0.70%]	[–2.0%, 1.1%]	[–12%, 16%]	[–20%, 20%]
	VSDDs in both stories	[–0.50%, 0.40%]	[–2.3%, 1.5%]	[–5.0%, 10%]	[–25%, 10%]
Biased	Conventional structure	[3.50%, 12.00%]	[–3.5%, 2.8%]	[–16%, 25%]	[–26%, 30%]
	VSDD in 1st story	[–5.00%, 10.0%]	[–2.5%, 3.0%]	[–18%, 27%]	[–46% , 34%]

Table 2 show the ranges for three times standard deviation of stiffness and damping estimate error. This is done for the different cases of the 2DOF shear building model. Note that all VSDD configurations in the 2DOF structure model, the number of estimations was 100 times with exact starting guesses and 26 times for with biased starting guesses.

4.4.2 Two Degree-of-Freedom Pier-Deck Bridge Model

The 2DOF bridge model shown in Fig. 11, provides an example that has full-scale structural parameters. A VSDD is attached between the deck and the pier as shown in Fig. 12 is assumed to provide an additional 0%, 10%, 20%, 30% and 40% stiffness; *i.e.*, $\kappa_1 = 0.0$, $\kappa_2 = 0.1$, ..., $\kappa_5 = 0.4$. Numerical quantities for this model, drawn from Erkus *et al.* (2002), are considered as an illustrative example $k_1 = 15.791$ MN/m, $k_2 = 7.685$MN/m, $m_1 = 100$ Mg (tons), $m_2 = 500$ Mg, $c_1 = 125.6$ kN·s/m, and $c_2 = 196$ kN·s/m. The experimental transfer functions are simulated in MATLAB by using the exact transfer functions plus the Fourier transform of a Gaussian pulse process typical of band-limited Gaussian white sensor noise vector processes. The noise induced in the experimental transfer function of the 2DOF bridge model is shown in Fig. 24, in both linear and log scales.

The iterative least-squares parametric frequency domain identification is performed on this 2DOF bridge model, both with a VSDD in the isolation layer between the deck and pier and without. The results show error reductions in both stiffness and damping estimates (though with the latter more modest than the former). The relative error in the stiffness estimates, shown in Fig. 25, have some small bias — about 0.5% in the estimate of the pier stiffness and about 2% in that of the isolator — that exists both with and without the VSDD (though the bias is to higher pier stiffness estimates with the VSDD, and lower without). While the bias is similar, the VSDD approach shows notable reductions in stiffness estimate variation, demonstrating that the VSDDs improve the identification. Similar observations may be made regarding damping estimates, as shown in Fig. 26. The VSDD approach slightly decreases the bias in the pier damping coefficient estimate, and modestly decreases the variation in both pier and isolator damping estimates.

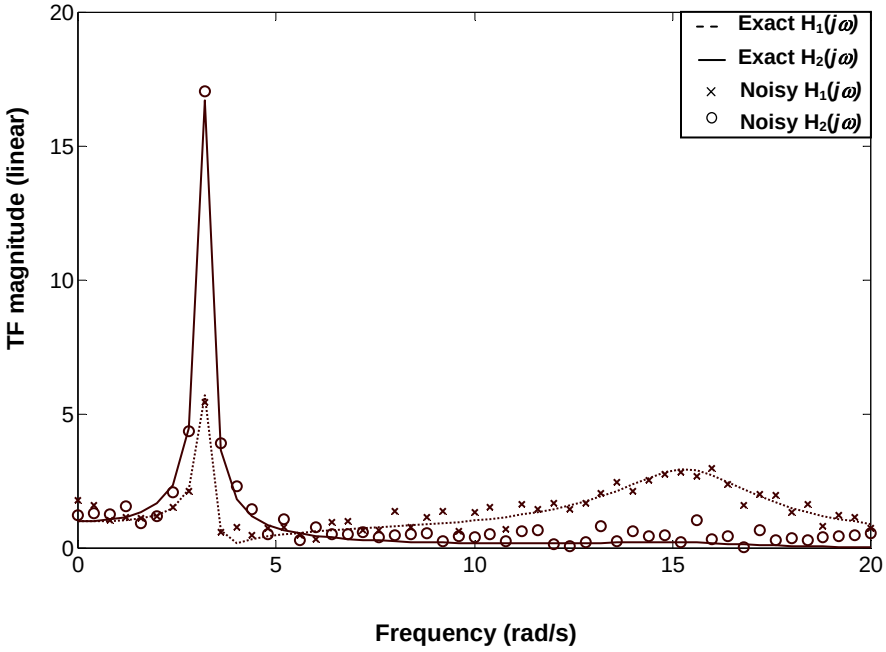

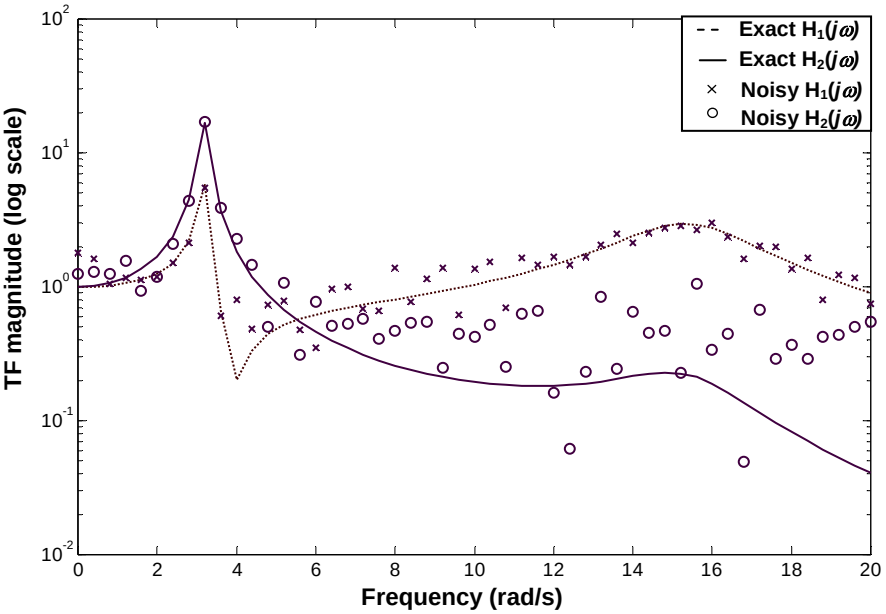

Figure 24. Exact and noisy TF magnitudes for 2DOF bridge model

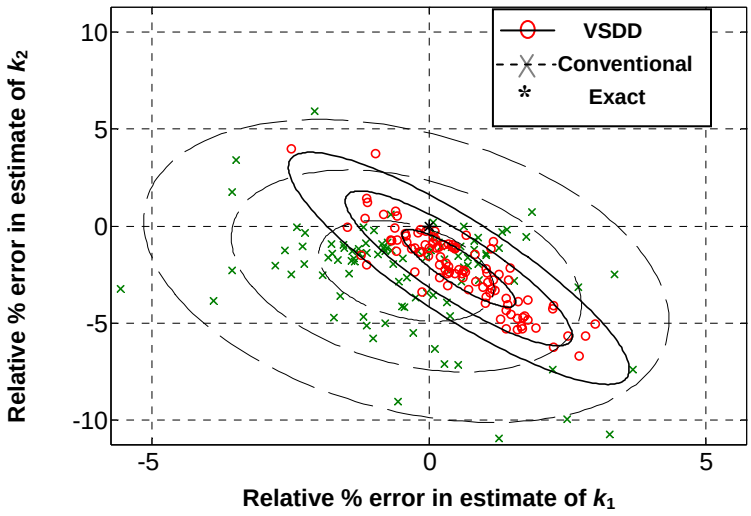

Figure 25. Stiffness estimate error levels for the iterative method with exact start in 2DOF bridge model

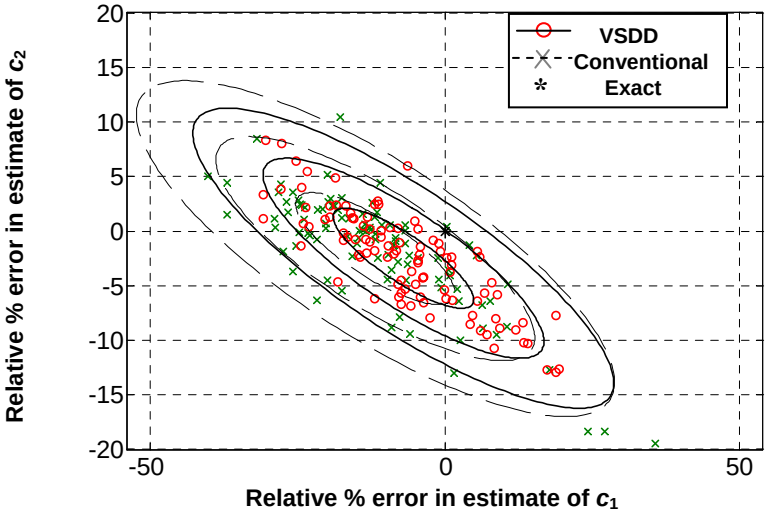

Figure 26. Damping estimates error levels for the iterative method with accurate start in 2DOF bridge model

4.4.3 Six Degree-of-Freedom Shear Building Model

The six degree-of-freedom structure has story and VSDD characteristics similar to the 2DOF building structure discussed previously. The story stiffnesses and floor masses are chosen, for simplicity, to be unity. The damping coefficient in each story is 0.05. There are three VSDDs in this structure, one in each of the first three stories, that can each provide five discrete stiffness levels that are 0, 10, 20, 30 and 40 percent of the story stiffness. The transfer functions are generated using the exact transfer function plus noise (shown in Fig. 27 for one noise realization), and the estimation is performed 20 times (each with a different random seed). In each estimation, the VSDD approach uses four sets of VSDD stiffness combinations: (0%,0%,0%), (10%,20%,30%), (20%,30%,10%), and (30%,10%,20%) in the first, second and third floors, respectively. As before, for fair comparison, the conventional structure approach uses four realizations of the transfer functions so that the amount of data is the same as the VSDD approach.

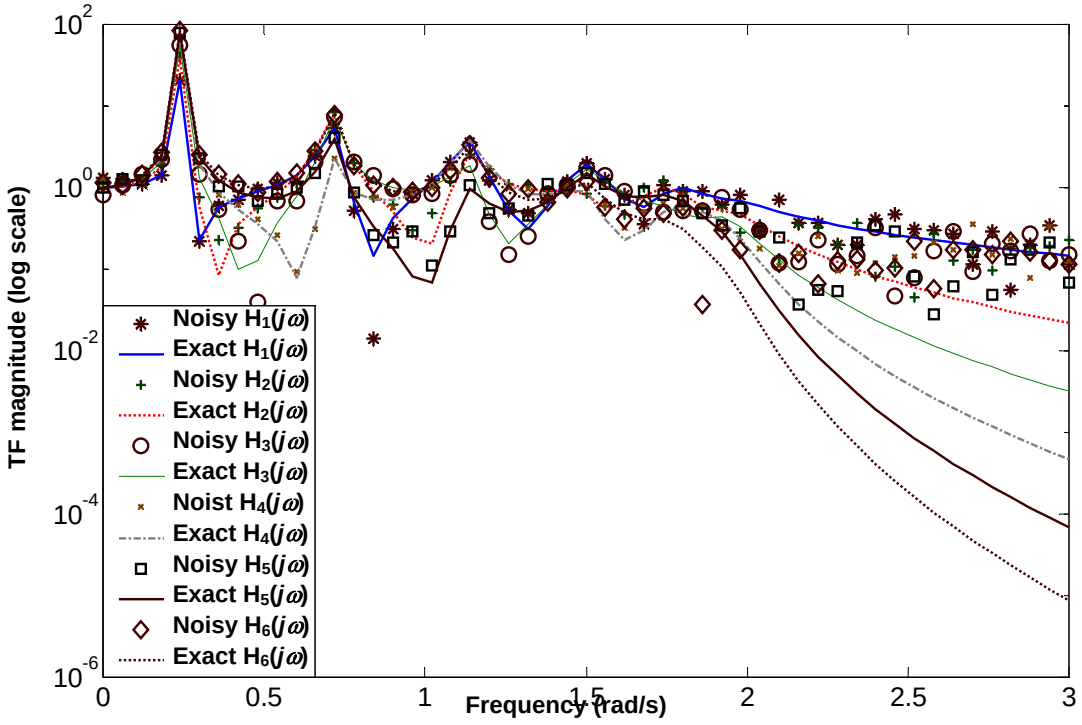

Figure 27. Exact and noisy TF magnitudes for 6DOF shear building model

Figure 28 shows the improvement in the estimates of the stiffness and damping coefficients when using VSDDs in the structural model. It is quite evident that the variations are dramatically reduced — up to 3 times for stiffness estimates and up to 4 times in the damping estimates. These results are similar to the improvements observed in lower-order 2DOF shear building model and the 2DOF bridge model. However, it can also be deduced that the expected improvements are more contrasted for higher degree of freedom models (*i.e.*, more complex models). The resulting estimates of the mean and the coefficient of variations for the stiffness and damping coefficients are shown in Table 3.

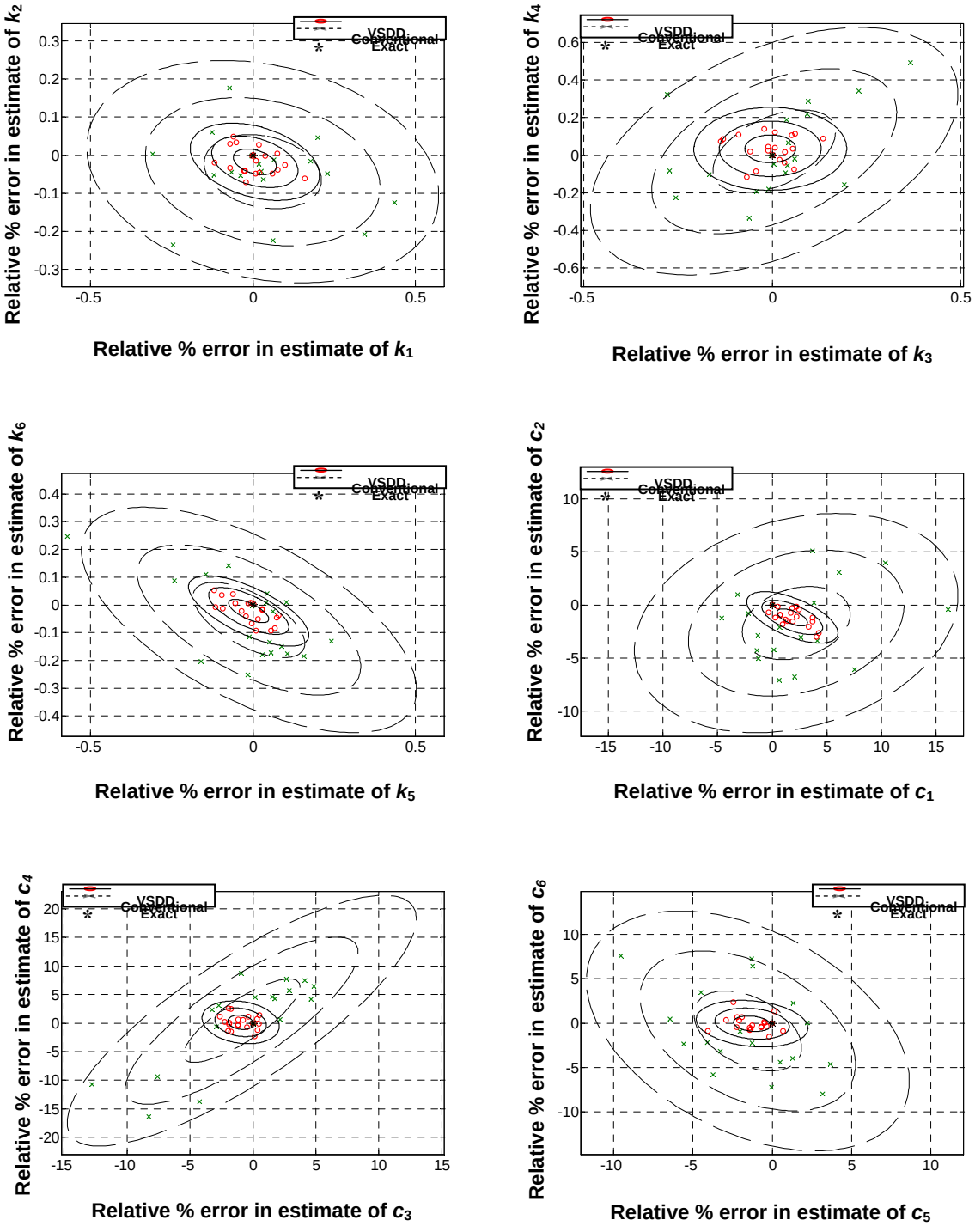

Figure 28. Stiffness and damping estimates error levels for the iterative method with exact starting guess in 6DOF model

Table 3. Estimate Means and Coefficients-of-Variation for 6DOF Shear Building Model

Variables	exact	coeff. of variation[%]			
		exact init. guess		*exact init. guess*	
		Conv. Struct.	VSDD	Conv. Struct.	VSDD
k_1	1.0	1.0003	1.0001	0.18	0.066
k_2	1.0	0.9996	0.9998	0.097	0.034
k_3	1.0	1.0001	0.9999	0.163	0.068
k_4	1.0	1.0002	1.0003	0.219	0.074
k_5	1.0	0.9999	0.9999	0.172	0.062
k_6	1.0	0.9995	0.9998	0.135	0.042
c_1	0.05	0.051095	0.05092	4.824	1.364
c_2	0.05	0.049145	0.049415	3.497	0.816
c_3	0.05	0.049555	0.049515	4.667	1.032
c_4	0.05	0.050210	0.050065	7.281	1.248
c_5	0.05	0.049230	0.049365	3.444	1.188
c_6	0.05	0.049560	0.049965	4.553	0.877

4.5 Using VSDDs with Variable Damping Only

Whereas the previous sections investigated the effects of VSDDs operating in a variable stiffness mode, it is possible that inducing added damping will have an effect on the SHM as well. Using variable damping would be of great interest since "smart" semiactive damping devices have received extensive study for vibration mitigation purposes (Soong and Spencer, 2002) and capitalizing on the synergies between control and SHM would be a cost-effective solution. In this example, the 2DOF bridge model is studied with a variable damping device in the isolation layer between the pier and deck. The damping levels of the device are 0%, 10%, 20%, 30%, and 40% of the isolator damping coefficient. As in the other numerical examples, the device is considered ideal (no internal device dynamics), the transfer functions are measured through standard means, and the least-squares parametric frequency-domain identification technique is applied.

The results, shown in Figs. 29 and 30, indicate that the *VSDD* approach, with the damping levels described above, did not differ significantly from the *conventional structure* approach. The relative error in stiffness estimates in Fig. 29 have similar bias in both approaches and a slightly larger variation with the VSDD damping device. Similar observations may be made about the damping estimates (Fig. 30).

One reason that the variable damping here did not provide any notable improvement is the very small force levels generated by the damping device. The damping forces in the isolation layer of this bridge model are about one order of magnitude smaller than the stiffness forces. As a result, changing the damping by this small amount has relatively little effect. Using larger force levels in the variable damper may overcome this difficulty and should be studied in the future.

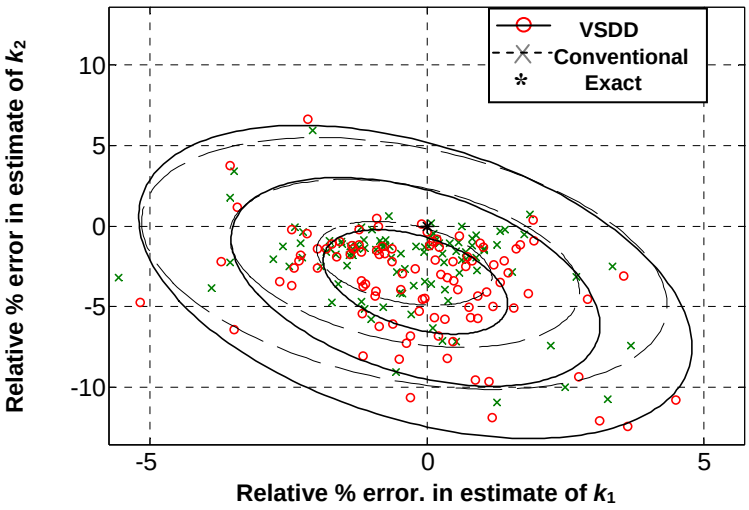

Figure 29. Stiffness estimates error levels for the iterative method with exact starting guess in bridge model with multiple variations of damping coefficients

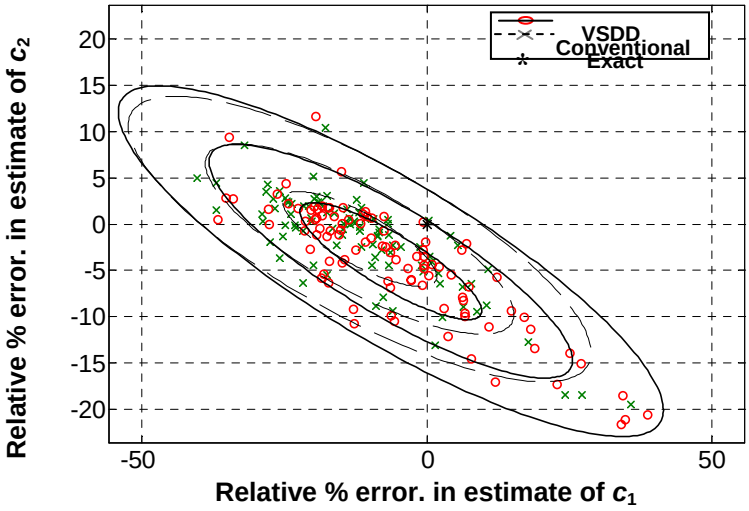

Figure 30. Damping estimates error levels for the iterative method with exact starting guess in bridge model with multiple variations of damping coefficients

5.0 CONCLUSIONS AND RECOMMENDATIONS

This report documents the initial study of the effectiveness of using variable stiffness and damping devices to improve estimates of structural parameters for structural health monitoring and damage detection. VSDDs are controllable passive devices that have been shown to have significant potential for mitigating structural response to natural hazards. This study demonstrates that VSDDs also have strong promise for use in SHM as well. Since VSDDs can be commanded to exert various force time histories, the response of a structure may be altered through the parametric changes effected by the VSDDs. The multiple "snapshots" of structural characteristics provided by the VSDD approach can provide additional information to make structural parameter identification more accurate and efficient.

This study investigated VSDD/SHM by identifying structural parameters — mass, stiffness and damping coefficients — based on measured absolute acceleration transfer function data, using a parametric frequency-domain least-squares identification method. For each numerical example and configuration, the structural parameters were identified, first with one or more VSDDs in the structure, and then with no VSDDs. In all cases, simulated sensor noise is added to the exact transfer function to replicate the noisy transfer functions that are typically obtained through standard experimental techniques. In each VSDD configuration, data is collected while the VSDDs are commanded to act in one of several discrete stiffness or damping modes, with different noise corrupting each subsequent data set. To make for a fair comparison, the conventional structure approach is provided with the same amount of data. The variation in identified structural parameters due to the effects of random noise are studied by performing these identifications a number of times, each with a different random seed to generate the noise, giving a measure of both the mean and the variance of the structural parameter estimates. While the VSDD approach is applicable to a wide variety of structural identification methodologies, it is herein studied in the context of a least-squares identification using the frequency-domain transfer function representation of the input/output dynamics of a structure. It is shown that one commonly-used simplification of this identification method gives biased results, and an alternate iterative approach is shown to give superior results. This iterative least-squares identification, with and without VSDDs, are applied to several numerical examples: a bridge pier/deck model and two shear building models. The VSDD is commanded to act as a discrete stiffness element or a discrete damping element, with stiffness or damping coefficient based on a fraction of the corresponding coefficient for the location where the VSDD is installed in the structure. When a VSDD acts as a discrete multi-level damping element with coefficient a fraction of that of the structure, little improvement is gained over the conventional structure approach, probably due to the very low force levels due to the VSDD damping. In contrast, the discrete stiffness behavior is shown to improve estimates of the stiffness and damping coefficients in the structure, particularly for the more complex numerical example with several VSDDs.

While the results herein definitely show that there is the potential for VSDDs to make a real contribution to structural health monitoring, a number of open questions and future directions have arisen in the course of this study. First, since the response to ambient excitation sources is, generally, quite low, the force levels of the VSDDs in this study were small — in fact, orders of magnitude smaller than the forces the structure is designed to withstand as well as, perhaps, two orders of magnitude smaller than the peak forces capable with current VSDD technology. Consequently, the VSDDs, especially in the discrete damping mode, were less

effective than would likely occur if they were commanded to use larger (but still moderate compared to the structural capacity) force levels. Future research should test if larger orce levels will give further improvement in identifying structural parameters. Second, VSDD behavior is commanded through a control system based on responses in the structure; for example, to act as a stiffness element with a particular stiffness level, the VSDD exerts a force proportional to the relative displacement across it. Herein, these devices were considered ideal and internal device dynamics were neglected. Future studies should examine the effects of VSDD device dynamics on the SHM improvements. Third, while it is convenient to consider (and explain) VSDDs in terms of the added stiffness and damping they provide, these concepts are inherently linear, time-invariant; and reliant only on local information rather, VSDDs can be commanded to exert a range of forces that change over time and cannot be characterized as either stiffness or damping or combination of the two. The challenge lies in developing a methodology for determining the best VSDD force time histories to improve the structural parameter estimation in an even more robust and efficient manner than studied herein.

Appendix A: Computational Procedure for 6DOF Shear Model

While using the symbolic math capabilities of MATLAB to formulate the iterative least-squares frequency-domain identification is convenient, it is not very efficient for larger problems, requiring the development of a semi-numerical solution procedure. The core of this alternate solution procedure lies in recognizing that the residual error $\hat{\mathbf{e}}_l$ in Eq. (11) can be separated into a set of numerical coefficients and a numeric representation of the symbolic unknowns. The r^{th} element of the $m\times 1$ error $\hat{\mathbf{e}}_l$ in Eq. (11) can be modified as

$$\hat{e}_{rl}(j\omega_i,\boldsymbol{\theta},\boldsymbol{\kappa}_k)=\frac{B_r(j\omega_i,\boldsymbol{\theta},\boldsymbol{\kappa}_k)-A(j\omega_i,\boldsymbol{\theta},\boldsymbol{\kappa}_k)\hat{H}_r(j\omega_i,\boldsymbol{\kappa}_k)}{\hat{A}_l(j\omega_i,\boldsymbol{\kappa}_k)}=\mathbf{c}_{rl}^{\mathrm{T}}(j\omega_i,\boldsymbol{\kappa}_k)\mathbf{v}_r(\boldsymbol{\theta}) \tag{A1}$$

where $\mathbf{c}_{rl}(j\omega_i,\boldsymbol{\kappa}_k)$ is an $n_{\mathbf{v}_r}\times 1$ vector of numeric coefficients of the corresponding elements of $\mathbf{v}_r(\boldsymbol{\theta})$, which themselves are each of the form

$$v_{sr}(\boldsymbol{\theta})=\prod_{i=1}^{n}\theta_i^{p_i^{rs}}\ ,\ s=1,\ldots,n_{\mathbf{v}_r}\ ,\ r=1,\ldots,m \tag{A2}$$

where the p_i^{rs} are non-negative integer exponents that can be arranged in $n\times 1$ vectors $\mathbf{p}^{rs}$ which can be collected into set $P_r=\{\mathbf{p}^{r1},\ldots,\mathbf{p}^{rn_{\mathbf{v}_r}}\}$. The symbolic $\mathbf{v}_r(\boldsymbol{\theta})$ is a function only of the unknown parameters and is different for each element of the transfer function error. The coefficient vector $\mathbf{c}_{rl}(j\omega_i,\boldsymbol{\kappa}_k)$ depends on the frequencies and the known parameters, and is different in each iteration and for each element of the transfer function matrix. Since the $\mathbf{v}_r(\boldsymbol{\theta})$ can be defined by the numeric exponents of the elements of the unknown $\boldsymbol{\theta}$, they can be stored and manipulated numerically just through the tensor p_i^{rs}.

Substituting Eq. (A1) into the square error Eq. (12), results in

$$\boldsymbol{\Delta}_l^2(\boldsymbol{\theta})=\sum_r\sum_i\sum_k\mathbf{v}_r^{\mathrm{T}}(\boldsymbol{\theta})\mathbf{c}_{rl}^{\dagger}(j\omega_i,\boldsymbol{\kappa}_k)\mathbf{c}_{rl}^{\mathrm{T}}(j\omega_i,\boldsymbol{\kappa}_k)\mathbf{v}_r(\boldsymbol{\theta}) \tag{A3}$$

where $(\cdot)^{\dagger}$ denotes complex conjugation. The order of summation and multiplication can be rearranged due to $\mathbf{v}_r(\boldsymbol{\theta})$ being independent of i and k, giving

$$\boldsymbol{\Delta}_l^2(\boldsymbol{\theta})=\sum_r\mathbf{v}_r^{\mathrm{T}}(\boldsymbol{\theta})\left[\sum_i\sum_k\mathbf{c}_{rl}^{\dagger}(j\omega_i,\boldsymbol{\kappa}_k)\mathbf{c}_{rl}^{\mathrm{T}}(j\omega_i,\boldsymbol{\kappa}_k)\right]\mathbf{v}_r(\boldsymbol{\theta}) \tag{A4}$$

The quantity in brackets is purely numerical and can be computed quite easily; let it be defined

$$\mathbf{C}_{rl}=\sum_i\sum_k\mathbf{c}_{rl}^{\dagger}(j\omega_i,\boldsymbol{\kappa}_k)\mathbf{c}_{rl}^{\mathrm{T}}(j\omega_i,\boldsymbol{\kappa}_k)\ ,\ r=1,\ldots,m \tag{A5}$$

which incorporates all of the information for the data frequency points $j\omega_i$ and the different sets of known parameters $\boldsymbol{\kappa}_k$.

The vectors $\mathbf{v}_r(\boldsymbol{\theta})$ are not all the same. It is convenient to define a single similar vector $\mathbf{v}(\boldsymbol{\theta})$ that contains all of the symbolic products of powers of all unknown $\boldsymbol{\theta}$ contained in the individual $\mathbf{v}_r(\boldsymbol{\theta})$.

$$v_s(\boldsymbol{\theta})=\prod_{i=1}^{n}\theta_i^{p_i^s}\ ,\ s=1,\ldots,n_{\mathbf{v}} \tag{A6}$$

where the p_i^s are non-negative integer exponents that can be arranged in $n_{\mathbf{v}}$ $n \times 1$ vectors $\mathbf{p}^s$ that can be collected as set $P = \{\mathbf{p}^1, \ldots, \mathbf{p}^{n_{\mathbf{v}}}\}$, which is the union of the individual sets for each element of the transfer function,

$$P = \bigcup_{r=1}^{m} P_r \tag{A7}$$

The individual symbolic vectors $\mathbf{v}_r(\boldsymbol{\theta})$ can be related to the global symbolic vector by

$$\mathbf{v}_r(\boldsymbol{\theta}) = \mathbf{T}_r \mathbf{v}(\boldsymbol{\theta}), \; r = 1, \ldots, m \tag{A8}$$

where $\mathbf{T}_r$ is a transformation matrix containing ones and zeros

$$\left[\mathbf{T}_r\right]_{is} = I(\mathbf{p}^{ri}, \mathbf{p}^s), \; r = 1, \ldots, m, \; i = 1, \ldots, n_{\mathbf{v}_r}, \; s = 1, \ldots, n_{\mathbf{v}} \tag{A9}$$

where $I(\mathbf{x}, \mathbf{y})$ is an indicator function that has value 1 when every element of $\mathbf{x}$ matches the corresponding element of $\mathbf{y}$.

Substituting Eqs. (A5) and (A7) into the square error Eq. (A4) gives

$$\boldsymbol{\Delta}_l^2(\boldsymbol{\theta}) = \sum_r \mathbf{v}^{\mathrm{T}}(\boldsymbol{\theta}) \mathbf{T}_r \mathbf{C}_{rl} \mathbf{T}_r \mathbf{v}(\boldsymbol{\theta}) \tag{A10}$$

which can be simplified since $\mathbf{v}(\boldsymbol{\theta})$ is independent of transfer function index r

$$\boldsymbol{\Delta}_l^2(\boldsymbol{\theta}) = \mathbf{v}^{\mathrm{T}}(\boldsymbol{\theta}) \left[\sum_r \mathbf{T}_r^{\mathrm{T}} \mathbf{C}_{rl} \mathbf{T}_r \right] \mathbf{v}(\boldsymbol{\theta}) = \mathbf{v}^{\mathrm{T}}(\boldsymbol{\theta}) \mathbf{C}_l \mathbf{v}(\boldsymbol{\theta}) \tag{A11}$$

where $\mathbf{C}_l$ is an $n_{\mathbf{v}} \times n_{\mathbf{v}}$ symmetric numeric matrix with elements c_{rs}^l. Computing these elements can be done quite efficiently; the slowest part is the process of forming the union of the exponent sets and building the resulting transformation matrices $\mathbf{T}_r$.

Determining the least-square estimates of the unknowns then requires the gradient of $\boldsymbol{\Delta}_l^2(\boldsymbol{\theta})$

$$\frac{\partial}{\partial \boldsymbol{\theta}} \left[\boldsymbol{\Delta}_l^2(\boldsymbol{\theta}) \right] = 2 \sum_{r=1}^{n_{\mathbf{v}}} \sum_{s=1}^{n_{\mathbf{v}}} c_{rs}^l v_r(\boldsymbol{\theta}) \frac{\partial v_s(\boldsymbol{\theta})}{\partial \boldsymbol{\theta}} \tag{A12}$$

and the elements of its corresponding Jacobian

$$\frac{\partial^2}{\partial \theta_i \partial \theta_j} \left[\boldsymbol{\Delta}_l^2(\boldsymbol{\theta}) \right] = 2 \sum_{r=1}^{n_{\mathbf{v}}} \sum_{s=1}^{n_{\mathbf{v}}} c_{rs}^l \left[v_r \frac{\partial^2 v_s}{\partial \theta_i \partial \theta_j} + \frac{\partial v_r}{\partial \theta_i} \frac{\partial v_s}{\partial \theta_j} + \frac{\partial v_r}{\partial \theta_j} \frac{\partial v_s}{\partial \theta_i} + \frac{\partial^2 v_r}{\partial \theta_i \partial \theta_j} v_s \right] \tag{A13}$$

The j^{th} element of the gradient can be simplified to a set of products of powers of unknowns and the corresponding coefficients

$$\frac{\partial}{\partial \theta_j} \left[\boldsymbol{\Delta}_l^2(\boldsymbol{\theta}) \right] = 2 \sum_{r=1}^{n_{\mathbf{v}}} \sum_{s=1}^{n_{\mathbf{v}}} \tilde{c}_{rs,j}^l \tilde{v}_{rs,j}(\boldsymbol{\theta}) \tag{A14}$$

where

$$\tilde{c}_{rs,j}^l = c_{rs}^l p_j^s \quad \text{and} \quad \tilde{v}_{rs,j}(\boldsymbol{\theta}) = \prod_{i=1}^{n} \theta_i^{p_i^r + p_i^s - \delta_{ij}} = \prod_{i=1}^{n} \theta_i^{\tilde{p}_{i,j}^{rs}} \tag{A15}$$

The elements of the Jacobian can be formed in a similar manner, resulting in a set of coefficients and exponents.

Equation (A14), then, is a nonlinear equation that is the linear combination of products of powers of the unknowns and can be solved through standard numerical root solving algorithms — this study used the function `fsolve( )` in MATLAB's Optimization Toolbox. The coefficients $\tilde{c}_{rs,j}^{l}$ and the exponents $\tilde{p}_{i,j}^{rs}$ can be computed in a purely numeric procedure from the assumed structural model, and the root solver is numerical. Thus, this alternate numerical solution avoids symbolic computation entirely. The result is that the 2DOF identification problems can be solved in a few seconds on a 2.4GHz Pentium 4, whereas a mostly symbolic computation takes on the order of several minutes on the same computer.

REFERENCES

Arizona Dept. of Transportation (ADOT) (2001). "Superstition Freeway," web page http://www.superstitionfreeway.com/

Au, S.K., K.V. Yuen and J.L. Beck (2000). "Two-Stage System Identification Results for Benchmark Structure." *Proceedings of the 14th ASCE Engineering Mechanics Conference*, Austin, Texas, 21–24 May 2000.

Beck, J.L. (1978). *Determining Models of Structures from Earthquake Records.* Report EERL78-01, California Institute of Technology.

Beck, J.L. (1990). "Statistical System Identification of Structures." In A.H-S. Ang, M. Shinozuka and G.I. Schueller (eds.), *Structural Safety and Reliability* (ASCE, New York)**,** 1395–1402.

Beck, J.L., B.S. May, and D.C. Polidori (1994a). "Determination of Modal Parameters from Ambient Vibration Data for Structural Health Monitoring." *First World Conference on Structural Control*, Los Angeles, California, 3–5 August 1994.

Beck, J.L., M.W. Vanik, and L.S. Katafygiotis (1994b)."Determination of Stiffness Changes from Modal Parameter Changes for Structural Health Monitoring." *First World Conference on Structural Control*, Los Angeles, California, 3–5 August 1994.

Beck, J.L., S. Au and M.W. Vanik (2001). "Monitoring Structural Health using a Probabilistic Measure." *Computer-Aided Civil and Infrastructure Engineering*, **16**, 1–11.

Béliveau, J.G., and S. Chater (1984). "System Identification of structures from Ambient Wind measurements." *Proceedings of the Eighth World Conference on Earthquake Engineering*, Prentice-Hall, Inc., Englewood Cliffs, New Jersey, 1984, **IV,** 307–314.

Bendat, J.S., and A.G. Piersol (2000). *Random Data: Analysis and Measurement Procedures*. Wiley, NY.

Bernal, D., and B. Gunes (2000). "Observer/Kalman and Subspace Identification of the UBC Benchmark Structural Model." *Proceedings of the 14th ASCE Engineering Mechanics Conference*, Austin, Texas, 21–24 May 2000.

Caicedo, J.M., S.J. Dyke and E.A. Johnson (2003). "NExT and ERA for Phase I of the IASC-ASCE Benchmark Problem: Simulated Data." *Journal of Engineering Mechanics*, ASCE, in press.

Capecchi, D., and F. Vestroni (1999). "Monitoring of Structural Systems by Using Frequency Data." *Earthquake Engineering and Structural Dynamics*, **28**, 447–461.

Chang, F.-K. (1999). *Structural Health Monitoring 2000. Proceedings of the 2nd International Workshop on Structural Health Monitoring*, Stanford University, 8–10 September 1999, Technomic Publishing Co., Lancaster, PA.

Corbin, M., A. Hera and Z. Hou (2000). "Locating Damage Regions Using Wavelet Approach." *Proceedings of the 14th ASCE Engineering Mechanics Conference*, Austin, Texas, 21–24 May 2000.

Doebling, S.W., C.R. Farrar, M.B. Prime and D.W. Shevitz (1996). "Damage Identification and Health of Structural and Mechanical Systems from Changes in their Vibration Characteristics: A Literature Monitoring Review." Los Alamos National Laboratory Report, LA-13070-MS, Los Alamos, New Mexico.

Doebling, S.W., C.R. Farrar and M.B. Prime (1998). "A Summary Review of Vibration-Based Damage Identification Methods." *The Shock and Vibration Digest*, **30**(2), 91–105.

Dyke, S.J., B.F. Spencer, Jr., M.K. Sain and J.D. Carlson (1996). "Modeling and Control of Magnetorheological Dampers for Seismic Response Reduction." *Smart Materials and Structures*, **5**, 567–575.

East Bay Business Times (EBBT) (2002). State Budget Deficit Could Hit $20 billion." Web page, 3 April 2002, http://eastbay.bizjournals.com/eastbay/stories/2002/04/01/daily48.html

Ehrgott, R.C., and S.F. Masri (1992). "Modelling the Oscillatory Dynamic Behaviour of Electrorheological Materials in Shear." *Smart Materials and Structures*, **1**(4)**,** 275–285.

Elmasry, M.I.S., and E.A. Johnson (2002). "Parametric Frequency Domain Identification in Multiconfiguration Structures." *15th ASCE Engineering Mechanics Conference (EM2002*), Columbia University, New York, 2-5 June 2002.

Erkus, B., A. Masato and Y. Fujino (2002). "Investigation of Semiactive Control for Seisimic Protection of Elevated Highway Bridges." *Engineering Structures*, **24**, 281–293.

Federal Highway Administration (FHWA) (2002). "National Bridge Inventory." Web pages, http://www.fhwa.dot.gov/bridge/britab.html

Gavin, G.P., R.D. Hanson and F.E. Filisko (1996a). "Electrorheological Dampers. Part I: Analysis and Design." *Journal of Applied Mechanics*, **63**, 669–675.

Gavin, G.P., R.D. Hanson and F.E. Filisko (1996b). "Electrorheological dampers. Part I: Testing and Modeling." *Journal of Applied Mechanics*, **63**, 676–682.

Hall, J.F., ed. (1995). "Northridge Earthquake of January 17, 1994, Reconnaissance Report." *Earthquake Spectra*, **11** supplement C.

Ho, B.L., and R.E. Kalman (1965). "Effective Construction of the Linear State-variable Models from Input/Output Data." *3rd Annual Allerton Conference on Circuit and System Theory*, 449–459; also *Regelungstechnik*, **14**, 545–548.

Housner, G.W., L.A. Bergman, T.K. Caughey, A.G. Chassiakos, R.O. Claus, S.F. Masri, R.E. Skelton, T.T. Soong, B.F. Spencer, Jr., and J.T.P. Yao (1997). "Structural Control: Past Present, and Future." *Journal of Engineering Mechanics*, ASCE, **123**,897–971.

Johnson, E.A., R.E. Christenson and B.F. Spencer, Jr. (2003). "Semiactive Damping of Cables with Sag." *Computer Aided Civil and Infrastructure Engineering*, **18**(2), 132–146.

Johnson, E.A., L.A. Bergman, P.G. Voulgaris (1997). *Online Modal State Monitoring of Slowly Time-Varying Structures*, NASA Contractor Report 198057.

Juang, J. (1994). *Applied System Identification*. Prentice Hall, Englewood Cliffs, New Jersey.

Juang, J., J.E. Cooper and J.R. Wright (1988). "An Eigen System Realization Algorithm Using Data Correlations (ERA/DC) for Modal Parameter Identification." *Control-Theory and Advanced Technology*, **4(**1), 5–14.

Juang, J., and R.S. Pappa (1985). "An Eigen System Realization Algorithm for modal Parameters Identification and Model Reduction." *Journal of Guidance*, **8**(5), 620–627.

Katafygiotis, L.S., and K. Yuen (2001). "Bayesian Spectral Density Approach for Modal Updating Using Ambient Data." *Earthquake Engineering and Structural Dynamics*, **30**(8) 1103–1123.

Katafygiotis, L.S., H.F. Lam and N. Mickleborough (2000). "Application of a statistical Approach on a Benchmark Damage Detection Problem." *Proceedings of the 14th ASCE Engineering Mechanics Conference*, Austin, Texas, 21–24 May 2000.

Kiremedjian, A.S. (1999). "Vulnerability and Damage of Structures from Earthquakes." Presentation." *Uncertaininty of Damageability Conference*, Risk Prediction Initiative, web page: http//:www.bbsr.edu/rpi/meetpart/Nov99

Kobori, T., and M. Takahashi (1993). "Seismic Response Controlled Structure with Active Variable Stiffness System." *Earthquake Engineering and Structural Dynamics*, **22**(12), 925–941.

Kurata, N., T. Kobori, S.M. Takahashi, T. Ishibashi, N. Niwa1, J. Tagami and H. Midorikawa (2000). "Forced Vibration Test of a Building With Semiactive Damper System." *Earthquake Engineering and Structural Dynamics*, **29**, 629–645.

Levy, E. (1959). "Complex Curve Fitting." *IRE Transactions on Automatic Control*, **AC-4**(1), 37–44.

Ljung, L. (1999). *System Identification: Theory for the User*, 2nd ed. Prentice Hall, Englewood Cliffs, New Jersey.

Luş, H., R. Betti and R. W. Longman (1999). "Identification of Linear Structural Systems Using Earthquake-Induced Vibration Data." *Earthquake Engineering and Structural Dynamics*, **28**, 1449–1467.

Luş, H., and R. Betti (2000). "Damage Identification in Linear Structural Systems." *Proceedings of the 14th ASCE Engineering Mechanics Conference*, Austin, Texas, 21–24 May 2000.

Makris, N, S.A. Burton, D. Hill and M. Jordon (1996). "Analysis and Design of ER Damper for Seismic Protection of Structure." *Journal of Engineering Mechanics*, ASCE, **122**(10), 1003–1011.

Mita, A. (1999), "Emerging Needs in Japan for Health Monitoring Technologies in Civil and Building Structures." In F.-K. Chang (ed.), *Structural Health Monitoring 2000: Proceedings of the 2nd International Workshop on Structural Health Monitoring*, Stanford University, 8–10 September 1999 (Technomic Publishing Co., Lancaster, PA), 56–67.

Moses, F., C.G. Schilling and K.S. Raju (1987). "Fatigue Evaluation Procedures for Steel Bridges." National Cooperative Highway Research Program, Report(**299)**, Transportation Research Board, National Research Council, Washington, DC, ISSN 0077-5614.

Nagarajaiah, S., and X. Sun (2003). "Base-Isolated FCC Building: Impact Response in Northridge Earthquake." *Journal of Structural Engineering*, ASCE, in press.

Nagarajaiah, S., and X. Ma (1996). "System Identification Study of a 1:10 Scale Steel Model Using Earthquake Simulator," *Proc. of Eng. Mech. Conf.,* ASCE, **2**, 764–767.

Patten, W.N., S. Jinghui, L. Guangjun, J. Kuehn and G. Song (1999). "Field Test of an Intelligent Stiffener for Bridges at The I-35 Walnut Creek Bridge." *Earthquake Engineering and Structural Dynamics,* **28**, 109–126.

Quek, S.T., W. Wang and C.G. Koh (1999). "System Identification of Linear MDOF Structures Under Ambient Excitation." *Earthquake Engineering and Structural Dynamics*, **28**, 61–77.

Rabinow, J. (1948). "The Magnetic Fluid Clutch." *AIEE Trans.*, **67**, 1308–1315.

Ramallo, J.C., E.A. Johnson and B.F. Spencer, Jr. (2002). "'Smart' Base Isolation Systems." *Journal of Engineering Mechanics*, ASCE, **128**, 1088–1099.

Ray, L.R., and L. Tian (1999). "Damage Detection in Smart Structures Through Sensitivity Enhancing Feed-back Control." *Journal of Sound and Vibration*, **227**(5), 987–1002.

Ribakov, Y., and J. Gluck (1999). "Active Control of MDOF Structures with Supplemental Electrorheological Fluid Dampers." *Earthquake Engineering and Structural Dynamics*, **28**, 143–156.

Sanayei, M.S., W. Doebling, C.R. Farrar, S. Wadia-Fascetti and B. Arya (1998). "Challenges in Parameter Estimation for Condition Assessment of Structures." *Structural Engineering World Wide*, *Proc. Structural Engineers World Congress*, San Francisco, CA, July 1998, Elsevier, New York, paper ref. T216-5.

Soong, T.T., and G.F. Dargush (1997). *Passive Energy Dissipation Systems in Structural Engineering*, Wiley & Sons, Chichester, England.

Soong, T.T., and B.F. Spencer, Jr. (2002). "Supplemental Energy Dissipation: State-of-the-Art and State-of-the-Practice." *Engineering Structures*, **24**, 243–259.

Spencer, B.F., Jr., G.Q. Yang, J.D. Carlson and M.K. Sain (1998). "Smart Dampers for Seismic Protection of Structures: a Full-Scale Study." *Proceedings of the 2nd World Conference On Structural Control*, Kyoto, Japan, 417–426.

Spencer, B.F., Jr., S.J. Dyke, M.K. Sain and J.D. Carlson (1997). "Phenomenological Model for Magnetorheological Dampers." *Journal of Engineering Mechanics*, ASCE, **123**(3), 230-238.

Spencer, B.F., Jr., and M.K. Sain (1997). "Controlling Buildings: A New Frontier in Feedback." *IEEE Control Systems Magazine*, **17**(6), 19–35.

Symans, M.D., and M.C. Constantinou (1997). "Seismic Testing of a Building Structure with a Semiactive Fluid Damper Control System." *Earthquake Engineering and Structural Dynamics*, **26**, 759–777.

Symans, M.D., and M.C. Constantinou (1999). "Semiactive Control Systems for Seismic Protection of Structures: a state-of the-art review." *Engineering Structures*, **21**, 469-487.

Takewaki, I., and M. Nakamura (2000). "Stiffness-Damping Simultaneous Identification using Limited Earthquake Records." *Earthquake Engineering and Structural Dynamics*, **29**, 1219–1238.

Vanik, M.W., J.L. Beck and S.K. Au (2000). "Bayesian Probabilistic Approach To Structural Health Monitoring." *Journal of Engineering Mechanics*, ASCE, **126**(7), 738–745.

Varadarajan, N., and S. Nagarajaiah (2000). "Semi-Active Variable Stiffness Tuned Mass Damper for Response Control of Wind Excited Tall Buildings: Benchmark Problem." *Proceedings of the 14th ASCE Engineering Mechanics Conference*, Austin, Texas, 21–24 May 2000.

Wang, C.S., and F.-K. Chang (1999). "Built-In Diagnostics for Impact Damage Identification of Composite Structures." In F.-K. Chang (ed.), *Structural Health Monitoring 2000: Proceedings of the 2nd International Workshop on Structural Health Monitoring*, Stanford University, 8–10 September 1999 (Technomic Publishing Co., Lancaster, PA), 612–621.

Winslow, W.M. (1949). "Induced Vibration of Suspensions." *J. Applied Physics*, **20,** 1137–1140.

Xu, Y.L.,W.L. Ku and J.M. Ko (2000). "Seismic Response Control of Frame Structures Using Magnetorheological/Electrorheological Dampers." *Earthquake Engineering and Structural Dynamics*, **29**, 557–575.

Yang, G., B.F. Spencer, Jr., J.D. Carlson and M.K. Sain (2002). "Large-Scale MR Fluid Dampers: Modeling and Dynamic Performance Considerations." *Engineering Structures*, **24**, 309-323.

Yang, J.N., J.C. Wu and Z. Li (1996). "Control of Seismic-Excited Buildings Using Active variable Stiffness Systems." *Engineering Structures*, **18**(8), 589–596.